

Dynamic branching in a neural network model for probabilistic prediction of sequences

Elif Köksal Ersöz, Pascal Chossat, Martin Krupa, Frédéric Lavigne

▶ **To cite this version:**

Elif Köksal Ersöz, Pascal Chossat, Martin Krupa, Frédéric Lavigne. Dynamic branching in a neural network model for probabilistic prediction of sequences. Journal of Computational Neuroscience, 2022, 50 (4), pp.537-557. 10.1007/s10827-022-00830-y . hal-03532787

HAL Id: hal-03532787

https://inria.hal.science/hal-03532787

Submitted on 18 Jan 2022

HAL is a multi-disciplinary open access archive for the deposit and dissemination of scientific research documents, whether they are published or not. The documents may come from teaching and research institutions in France or abroad, or from public or private research centers.

L'archive ouverte pluridisciplinaire **HAL**, est destinée au dépôt et à la diffusion de documents scientifiques de niveau recherche, publiés ou non, émanant des établissements d'enseignement et de recherche français ou étrangers, des laboratoires publics ou privés.

Abstract

An important function of the brain is to adapt behavior by selecting between different predictions of sequences of stimuli likely to occur in the environment. The present research studied the branching behavior of a computational network model of populations of excitatory and inhibitory neurons, both analytically and through simulations. Results show how synaptic efficacy, retroactive inhibition and short-term synaptic depression determine the dynamics of choices between different predictions of sequences having different probabilities. Further results show that changes in the probability of the different predictions depend on variations of neuronal gain. Such variations allow the network to optimize the probability of its predictions to changing probabilities of the sequences without changing synaptic efficacy.

Dynamic branching in a neural network model for probabilistic prediction of sequences

Elif Köksal Ersöz[1,2], Pascal Chossat[2,3], Maciej Krupa[2,3], and Frédéric Lavigne[4]

[1]Univ Rennes, INSERM, LTSI - UMR 1099, Campus Beaulieu, 35000 Rennes, France
[2]Project Team MathNeuro, INRIA-CNRS-UNS, 2004 route des lucioles, 06902 Sophia-Antipolis, France
[3]Université Côte d'Azur, Laboratoire Jean-Alexandre Dieudonné, Campus Valrose, 06102 Nice cedex 2
[4]BCL, UMR CNRS-UNS, 25 avenue François Mitterrand, 06300 Nice Cedex 4

January 18, 2022

1 Introduction

1.1 Prediction of sequences

An important function of the brain is to adapt behavior to a world whose structure changes over space and time. A way to adapt to the sequences of stimuli that occur in the environment is to use stored knowledge to predict which stimuli are likely to occur Bastos2020 given that prediction improves stimulus perception and visuomotor integration [HG12, BSM$^+$16, KW04]. Neurophysiological studies on behaving nonhuman primates have shown that neurons coding for a stimulus that is expected given a preceding one are activated before the stimulus onset [Miy88, Mil99, ED99]. Neurons recordings have shown that neurons activated by the first stimulus remain in retrospective activity after its offset [Miy88, MC88, FA71]. In the mean time, neurons that code for the expected second stimulus exhibit an elevated firing rate before the onset of the second stimulus and respond strongly to it [Miy88, MC88, NYM01, YNM03, ED99, RRM99]. Such prospective activity reveals associative priming that allows prediction of a stimulus given the preceding sequence [WAM01, WM03, BKW$^+$03, MWM06] (see [BSM$^+$16]), as a

function of the learned association between the stimuli [GCD+94, MSZA01, SM91, WYF+03, IQF15]. The benefits of successful predictions are shorter processing times and decreased error rates, reported in both nonhuman primates [ED99] and in humans [ALA+19, LVd00, HHNT14, Nee91]. Predictions are also reported to modify the EEG, fMRI and MEG signals in humans [DUK05, KDS11, WFN+15, DMZ+15].

Biologically inspired models of the cerebral cortex have proposed synaptic efficacy between populations of neurons as a critical parameter that allows the retrospective activity of neurons coding for a first stimulus to trigger prospective activity of neurons coding for the predicted stimulus [LD02, Lav04, MAB03, BL09]. Previous work has identified conditions on the connectivity matrix for a neural network to generate sequences of several items predicted in memory [ACKL17, CM20]. This research studied sequence generation in which the network faced two-ways choices to select one or the other direction along a *single* sequence. However, complex environments confront the brain with prediction among multiple sequences and with decision making regarding which sequence to predict. These complex processes raise the question of the necessary and sufficient conditions for the network to make crucial types of three-ways or more choices. The present research was therefore interested in understanding how neural, synaptic and network properties determine the dynamics of N-ways choices in a computational network model of populations of excitatory and inhibitory neurons.

1.2 Probabilistic prediction

Different environments can have variable levels of predictability depending on the probabilities of the sequences of stimuli. On the one hand, an environment made of always the same sequences of events would be fully predictable and learning would not need memory updating. On the other hand, an environment made of always different sequences would not be predictable at all and random memory updating could not allow the adaptation of behavior. In between these subcritical and supercritical environments, critical environments are made up of sequences of various levels of probability [Chi10, BP95, BC01]. In such complex environments, in a given context events can happen with their own probability, hence raising a N-ways decision problem of which one to predict. For example, a leopard (system) hunting prey (context) may expect to eat quietly (first possibility) or be disturbed by scavengers (second possibility). Priming studies in humans [LML21] and nonhuman primates [MFR16] indicate that the brain activates items in memory as a function of previous learning of their transitional probability given by correlation of the stimuli in the learned sequences. In turn, the magnitude of the activation of the predicted items increases with the learned correlation [VP14, LVP14, LDC+12, LCDV13]. The relationship between prediction and learning is studied by biologically inspired models of the cerebral cortex, which show that the more probable a sequence during

learning, the more potentiated the synapses between the populations of neurons coding for the items and the stronger the activation during prediction [MAB03, BL09, LDC+12, LCDV13, LAD14, Wan02].

To investigate the behavior of a neural network able to select between different sequences to predict, the present study considered the dynamic changes of network states in its state space. A *state* of the network is characterized by the level of activity of its neurons: a fraction of them show a high level of activity while the others stay at rest. The state space describes how all possible states of the network are connected together and can follow each others when the network changes state. The reciprocal dynamic activation or inhibition between populations of neurons coding for items in memory are generally assumed to subtend fundamental cognitive processes such as working memory, associative priming and pathological behaviors [BW01, LDD11, MAB03, ACKL17, LD08, RLDW08]. Within this framework, memorized item are encoded by states of the network in which only a fraction of the populations of neurons is activated. Modeling approaches indicates that the connectivity matrix between the populations of neurons determines both the content of stable states, in terms of which populations are active or inactive for this state and the possibility of transition between states, or priming, in terms of which populations will change their level of activation [ABT94, AB97, Bru96, CM20, Hop82] (Fig. 1a).

Within this framework, cognitive processes are described as sequences of network states within the state space. Complex network behavior triggered by a stimulus would then require that some populations of neurons become activated/inhibited in sequences that can be long and complex. As a consequence the network should be able to navigate within its state space by taking paths at different elementary types of states ranging from 1-way states (at the end of a branch) to N-ways branching states (connected to N different states, see Fig. 1b). By navigating in the state space, the network in a given branching state can either remain stable or change to one of the connected states. The 'choice' depends on which populations are activated or inactivated, which depends in turn on synaptic efficacy between these populations. A simple process of state change corresponds to priming and prediction in terms of the activation of a sequence of states before the sequence of stimuli. Recent studies have investigated how priming from close to close between associated neurons populations generates sequences of learned states along a simple chain of connected states [KEAC+20].

1.3 Prediction changes

The mechanisms of activation of sequences of states make possible predictions adapted to the variable level of probability of the stimuli that could occur following a given context. For example, the leopard could make predictions as a function of the relative likelihood of eating quietly or being disturbed. However, organisms usually alternate between multiple *local* en-

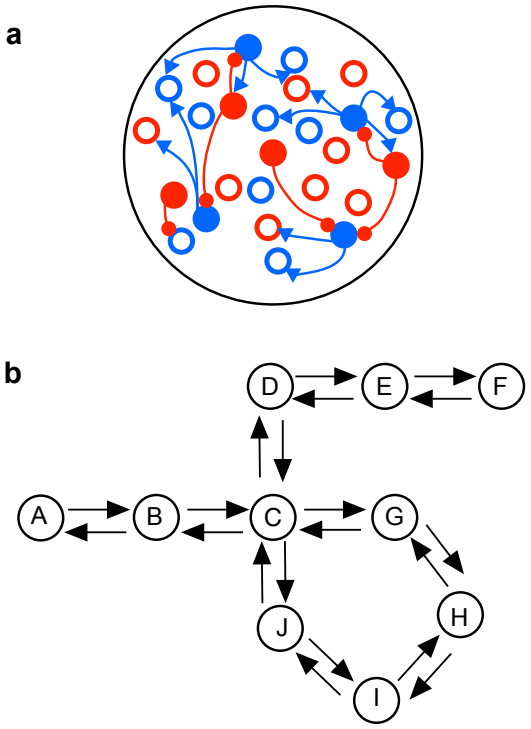


Figure 1: **a** A state of the network (black circle) corresponds to the activation (filled circles) or inhibition (empty circles) of populations of excitatory (blue) neurons and of inhibitory (red) neurons. **b** Example of a network of states ξ^N in the state space made of of 1-way (ξ_1), 2-ways (ξ_2), 3-ways (ξ_3) and 4-ways (ξ_4) branching states.

vironments between which the probabilities of the sequences of events are different. For example, despite a higher average probability of eating quietly, the probability of being disturbed can transiently become higher. The flexible adaptation of behavior to those alternations therefore requires rapid adaption of predictions to the current environment without forgetting knowledge on the preceding one. This points to the question of changing predictions without changing knowledge on the sequences embedded within the connectivity matrix.

A recent computational model by [KEAC$^+$20] has presented a network that could either reproduce regularly the same sequence of states in the forward direction or generate different sequences by alternating irregularly forward and backward steps. This was realized for a *fixed* learned connectivity matrix thanks to variations in neuronal gain, along with short-term synaptic depression and neuronal noise. Such mechanism could be involved in switching the brain behavior between either repeating reliable sequences

[VCSJK15, CC01, BM05, ED12, XJP12] or creating new sequences [BAHS08, CGS+09, Gui50, ABOY12, FB12, GYdSL+13]. The ability of organisms to reproduce previous actions or to explore new actions is thought to rely on the neuromodulation of the gain of cortical neurons [AC05, Kri08]. For example, dopaminergic neuromodulation of the prefrontal cortex [LKD+07] has been proposed to modify the choice for new actions [RG06]. Further, modulation of the neuronal gain is reported to impact network dynamics such as in working memory [BW01], episodic memory [LR14] and more generally the functioning of brain networks [RLDW08]. More specifically in the case of associative priming [LD08] have reported that the difference of activation of strong and weak associates to a cue was varied by changing neuronal gain. This later model points to the role of neuronal gain in the selection of sequences of variable probability, but it did not allow for the activation of long sequences.

1.4 Objectives of the study

The present research analyzed the behavior of neural networks of excitatory and inhibitory populations of neurons in the selection of branches in N-ways choices between learned states. This is a development from [KEAC+20] where sequential activation of states (2-ways choices) was analyzed. This behavior was referred to as *latching dynamics* in previous studies [Tre05, RNTK08, LBS12]. The novelty of our approach was that we were able to perform a rigorous mathematical analysis of the dynamics by considering the "jumps" from one state to the next as a dynamic bifurcation in a two-time-scale system of differential equations, in which the fast time scale corresponded to neurons spike rate and the slow time scale corresponded to synaptic short term depression (STD, [TM97, VSG+97]). Our model is defined in Section 2. More details about the mechanism of occurrence and conditions of latching dynamics are given in the appendix. Simulations on two examples of neural networks with 3-ways and 4-ways branchings have tested the effects of biologically plausible synaptic and neural parameters - synaptic connectivity, feedback inhibition and neuronal gain - on the dynamics. We further investigated the effect of neuronal gain on the ability of the network to switch behavior between predicting the most probable sequence according to previous learning and predicting a less probable state to quickly adapt to changes in the environment. These numerical results are exposed in Section 3.

2 The model

The model presented here investigates N-ways branching behavior in a model of excitatory and inhibitory populations of neurons. Our approach regarding 2-ways branchings was first exposed in [ACKL17] and further developed

in [KEAC$^+$20]. It is related to the model of semantic priming leading to latching dynamics developed by Lerner, Bentin and Shriki [LBS12].

2.1 The basic equations

The model consists in a network of N "units" which are characterized by an activity variable $x_i \in [0,1]$, $i = 1, \ldots, N$. Units should be thought of as populations of highly interconnected neurons and x_i is the averaged and normalized output pulse rate of unit i. The transfer function from the averaged membrane potential u_i to x_i is modeled by the logistic map $x = S(u) = (1 + e^{-\gamma u})^{-1}$. The coefficient γ is the gain of the units. The connection from unit j to unit i is characterized by a coefficient J_{ij} that corresponds to the learned synaptic efficacy [Heb49, BL73, BC93, KB94]. Such strength of the connection between populations is reported as an essential parameter to code the relation between stimuli in memory [YFEE98, Wei98]. We take into account that When a neuron j is active, the neurotransmitter release at the synapses of this neuron "saturates", so that the strength J_{ij} diminishes via STD proportionally to the neurons firing rate [TM97, VSG$^+$97]. Synaptic efficacy recovers when the neuron becomes inactive. We write $J_{ij} = J_{ij}^{max} s_j$ where J_{ij}^{max} are the coefficients of the connectivity matrix J^{max} resulting from a Hebbian learning process and s_j vary according to the rule established by [TM97], which we write

$$\tau_r \dot{s_i} = 1 - s_i - \rho s_i x_i \tag{1}$$

where τ_r is the time constant of the synapse's recovery and $\rho = \tau_r U$, U being the fraction of used synaptic resources. For an active unit with initially maximal synaptic strength $s_i = 1$, s_i decays towards the value $S = (1 + \rho)^{-1}$.

Following [LBS12], we now write the equation for u_i (with slightly different notations) by using Amari's formulation for the averaged membrane potential [Ama72], which is known to be mathematically equivalent to Wilson-Cowan formulation [WC12] for the averaged firing rate (see [MF12]):

$$\dot{u_i} = -u_i + \sum_{j=1}^{N} J_{i,j}^{max} s_j x_j - \lambda \sum_{j=1}^{N} x_j - I + \eta \tag{2}$$

where I is a constant non-selective inhibition on all populations of excitatory neurons due to spontaneous activity of inhibitory neurons, partly due to external noise and independent of the activity of excitatory neurons in the network [ABT94, AB97, BW01]. This type of inhibition determines the 'computational' distance of the population activity to the excitability threshold. The parameter λ is a variable non-selective feedback inhibition on all populations of excitatory neurons. It corresponds to the activation of inhibitory neurons proportional to the level of activation of all populations of

excitatory neurons in the network. Such non-selective inhibitory retroaction is made possible due to long-range connection from excitatory neurons onto inhibitory interneurons. The term η expresses a noise input to each population of excitatory neurons.

Now, as postulated in [LBS12] and other studies, in the absence of synaptic depression the learned memory items are stored in the form of attracting steady-states of (2) such that the activity of the i-th unit is either $x_i = 0$ (resting state unit) or 1 (fully excited unit). We call these steady-states of the network the *learned patterns*. Single cell recordings and local field potentials report that neurons in the macaque cortex respond to several different stimuli [RT95, TT01, TFTL06] and that a given stimulus is coded by the activity of a population of neurons [HKP05, YY92, KHK$^+$06]. The coding of stimuli in the model is then distributed across a pattern of activity of neural populations [QK10, Qui16]. Two different but related stimuli then share some active neurons populations, whose relation is coded by the overlap in the populations responsive to the stimuli [FNK$^+$10, Qui12]. Retrieving memory occurs when a cue puts the network in a state which belongs to the basin of attraction of the learned pattern. The learning process associated to these patterns shapes the connectivity matrix $(J_{ij})_{i,j=1\cdots N}$ through a simplified version of the learning Hebbian rule introduced in [Tso90] (see [ACKL17] for details), which we write for P learned patterns as

$$J_{i,j}^{max} = \sum_{p=1}^{P} \xi_i^p \xi_j^p \tag{3}$$

Here ξ_i^p denotes the i-th component of the p-th pattern being learned by the network.

It appears to be more convenient for our purpose to replace Eq. (2) by the corresponding equation for the activity variable x_i. A simple calculation shows that the deterministic part of (2) is then replaced by

$$\begin{aligned} \dot{x_i} =& \gamma x_i(1-x_i)(-S^{-1}(x_i) + \sum_{j=1}^{N} J_{i,j}^{max} s_j x_j \\ & - \lambda \sum_{j=1}^{N} x_j - I) \end{aligned} \tag{4}$$

where $x_i \in (0,1)$. The r.h.s of (4) formally vanishes whenever $x_i = 0$ or 1. At least formally, any trajectory of the system (4) with initial point on a face, an edge or a vertex of the cube $[0,1]^N$ lies entirely in this face, edge or vertex. In particular the vertices of the cube are steady-states and remark that learned patterns are precisely located on vertices. Unfortunately the term $S^{-1}(x_i)$ is singular at 0 and 1: it diverges at these values. In [ACKL17] this problem was circumvented by replacing the function $S^{-1}(x)$ at $x = 1/2$ by its Taylor expansion at some arbitrary order. This approximation is mathematically

justified because the power series converges uniformly on any interval in $(0, 1)$. When this is done, the new system of ODEs (ordinary differential equations) is now well-defined on the cube $[0, 1]^N$ and the geometry of this system makes the analysis of the dynamics near and between learned patterns much simpler.

For our purpose, which is to give a qualitative description of the mechanism by which latching dynamics occurs between learned patterns, a first order approximation of S^{-1} is good enough. Note that, $S^{-1}(x) \sim (4x-2)/\gamma$. Choosing this approximation in (4), we arrive, after rescaling time with γ and incorporating $-2/\gamma$ in the global inhibition term I, to the equation

$$\begin{aligned} \dot{x_i} =& x_i(1-x_i)(-\mu x_i + \sum_{j=1}^{N} J_{i,j}^{max} s_j x_j \\ & - \lambda \sum_{j=1}^{N} x_j - I) + \eta \end{aligned} \tag{5}$$

where now $\mu = 4/\gamma$. Hence up to a factor 4, μ is the inverse of the unit's gain. For the rest of the paper μ instead of γ will be the parameter characterizing the units. The term η represents a noise that can be thought of as a fluctuation of the firing rate due to random presence or suppression of spikes. In our simulations, η follows a uniform distribution and we make sure that the perturbations due to η are positive for firing rates near 0 and negative for firing rates near 1. Equations (5), (3) and (1) define the model introduced in [KEAC$^+$20] for latching dynamics in neural networks. A comparison of simulations of latching dynamics exhibited by (4) and (5) confirms the relevance of this approximation/simplification.

2.2 Chains and graphs of learned patterns

We now specify conditions which we put on learned patterns. These conditions have to be simple enough to allow for a mathematical analysis of the system, yet being able to enlighten a general mechanism for latching dynamics among a set of learned patterns. With this in mind, we assume that the matrix J^{max} is derived by the application of the learning rule (3) to a collection of learned patterns with only two non zero entries (*i.e.* two active populations of neurons), which therefore have the general form

$$\xi = (0, \ldots, 0, 1, \ldots, 0, 1, 0, \ldots, 0), \tag{6}$$

where the two excited units are placed at ranks $p < q \leq N$. Now, as mentioned in the previous section, different patterns corresponding to related stimuli show some common active units, which we denote as an *overlap* between these patterns. Let $\mathcal{P}$ be a subset of the set formed by these patterns, which satisfies the following additional two conditions:

(**H1**) Any pattern in $\mathcal{P}$ has one common (overlapping) excited unit with at least one other pattern in $\mathcal{P}$;
(**H2**) any two patterns in $\mathcal{P}$ can be connected via a sequence of overlapping patterns.
Therefore $\mathcal{P}$ forms a connected graph. In [KEAC$^+$20] it was further assumed that $q = p+1$, henceforth reducing the graph to a single chain of overlapping units $\xi^1 \to \xi^2 \cdots \to \xi^P$ where $\xi^1 = (1, 1, 0, \ldots, 0), \ldots, \xi^P = (0, \ldots, 1, 1)$. In this case,

$$J^{max} = \begin{bmatrix} 1 & 1 & 0 & \ldots & 0 \\ 1 & 2 & 1 & \ddots & \vdots \\ 0 & \ddots & \ddots & \ddots & 0 \\ \vdots & \ddots & 1 & 2 & 1 \\ 0 & \ldots & 0 & 1 & 1 \end{bmatrix}_{N \times N} . \tag{7}$$

It was shown in [KEAC$^+$20] that noise was sufficient to produce latching dynamics of the system (5)-(1) such that if the initial condition is set close to ξ_1, the trajectory "jumps" sequentially from one pattern to the next: $\xi^1 \to \xi^2 \to \cdots$. The mechanism for this particular dynamics is recalled in Appendix A. Depending on parameter values and specifically on μ, the latching dynamics can continue forward, stop or change direction and go in the reverse order. Note that, by a simple argument of symmetry in the equations and in the connectivity matrix, starting from ξ^P instead of ξ^1 would lead to a sequence in the reverse order.

Remark 1. The fact that any two consecutive patterns in the sequence share one active unit was the key ingredient in [KEAC$^+$20] to produce sequential dynamics. We call *regular activation* the switch between two patterns sharing one active unit. It does not however exclude the possibility that the dynamics 'jumps' over one pattern (or more) in the sequence.

Remark 2. The last pattern ξ^P (or ξ^1 if the dynamics goes in reverse order), cannot usually be reached because the first and last diagonal elements in (7) are smaller than the other diagonal elements, which implies that there is not enough synaptic strength to excite the last unit (or the first one for a backward sequence).

In the present work we aim at generalizing the results of [KEAC$^+$20] N-ways branching ($N > 2$) by relaxing the sequential condition $q = p+1$. The new feature in this case is that branching of several chains can occur (N-ways branching) at the nodes of the graph at which more than two patterns overlap, which means that more than two edges, or branches, emanate at these nodes We call such nodes *multiple nodes* of the graph. We address the question of what happens in this case. What are the conditions for latching dynamics to continue on a branch beyond the branching point and if so, what are the parameters that determine the selection of a branch over the other? We note that the number of possible connected graphs $\mathcal{P}$ with a given number P of

patterns increases quickly with P. In Section 3 we shall explore in details relatively simple situations, but there are arguments to support the idea that the phenomena we have observed can be generalized to more complicated graphs. For the rest of this section we discuss some general properties of these graphs of learned patterns with overlap.

Proposition 1. *Given a connected graph $\mathcal{P}$ with P learned patterns satisfying (H1-H2), the minimal number of neurons necessary to realize this network is $P+1$ if at least one node has only one connection to another node and is P otherwise.*
Then the connectivity matrix calculated with formula (3) *has the following property: the diagonal coefficient $J_{i,i}^{max}$ is equal to the number d of patterns in which the unit x_i is active. All other coefficients $J_{i,j}$ have value 1 if there exist a pattern with active units at places i and j, and 0 otherwise.*

Proof. This is a straightforward consequence of formula (3). □

Example 1. *Consider first the graph in Fig.2, with patterns $\xi^1 = (1,1,0,0,0,0,0)$, $\xi^2 = (0,1,1,0,0,0,0)$, $\xi^3 = (0,0,1,1,0,0,0)$, $\xi^4 = (0,0,0,1,1,0,0)$, $\xi^5 = (0,0,1,0,0,1,0)$, $\xi^6 = (0,0,0,0,0,1,1)$. The connectivity matrix in*

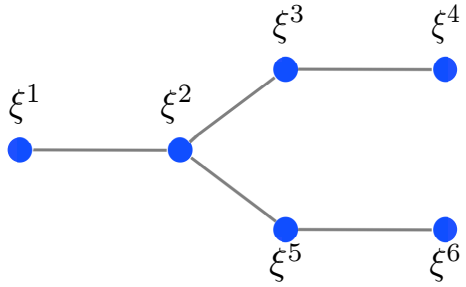


Figure 2: Example of a graph $\mathcal{P}$ connecting 6 learned patterns.

this case is

$$J^{max} = \begin{bmatrix} 1 & 1 & 0 & 0 & 0 & 0 & 0 \\ 1 & 2 & 1 & 0 & 0 & 0 & 0 \\ 0 & 1 & 3 & 1 & 0 & 1 & 0 \\ 0 & 0 & 1 & 2 & 1 & 0 & 0 \\ 0 & 0 & 0 & 1 & 1 & 0 & 0 \\ 0 & 0 & 1 & 0 & 0 & 2 & 1 \\ 0 & 0 & 0 & 0 & 0 & 1 & 1 \end{bmatrix} \tag{8}$$

Example 2. *We now impose a connection between ξ^4 and ξ^6 in Fig.2. Then six units are enough to realize the graph $\mathcal{P}$, with patterns $\xi^1 = (1,1,0,0,0,0)$,*

$\xi^2 = (0,1,1,0,0,0)$, $\xi^3 = (0,0,1,1,0,0)$, $\xi^4 = (0,0,0,1,1,0)$, $\xi^5 = (0,0,1,0,0,1)$, $\xi^6 = (0,0,0,0,1,1)$. *The connectivity matrix reads*

$$J^{max} = \begin{bmatrix} 1 & 1 & 0 & 0 & 0 & 0 \\ 1 & 2 & 1 & 0 & 0 & 0 \\ 0 & 1 & 3 & 1 & 0 & 1 \\ 0 & 0 & 1 & 2 & 1 & 0 \\ 0 & 0 & 0 & 1 & 2 & 1 \\ 0 & 0 & 1 & 0 & 1 & 2 \end{bmatrix} \tag{9}$$

Note that, all diagonal coefficients have values ≥ 2 except the first one. This is because now ξ^4 and ξ^6 have an overlap, which results in a closed chain $\xi^2 \to \xi^3 \to \xi^4 \to \xi^6 \to \xi^5 \to \xi^2$. We call loop a chain which closes on itself.

2.3 The extended equations

The dynamics in the case of a single chain has been analyzed in details in [KEAC$^+$20]. We expect similar behavior for a loop (a chain closing back to itself), with a possibility that the latching dynamics be cycling in this case.

If now a multiple node is encountered in the chain, one can intuitively expect that the dynamics will continue along one or another of the branches following that node, with equal chances for the choice of the branch. Indeed in the equations as well as in the connectivity matrix J^{max}, no preference exists for one branch rather than another. This expectation is confirmed by numerical simulations unless some inhomogeneity is introduced in the parameters or in the coefficients of J^{max}. This will be shown in Section 3, on two specific graphs extending examples 1 and 2 for a system with 10 units.

We note here that according to the learning rule, the diagonal coefficient of J^{max} at a unit is proportional to the number of branches to the node that contains this unit. As a consequence, whenever this unit is excited it will remain so forever despite synaptic depression, hence prohibiting latching dynamics to continue beyond the nodes which have this unit excited. Note that this phenomenon would not be observed in example 1 (Fig. 2). Indeed the nodes ξ^4 and ξ^6 (at which the third unit has relaxed to 0) cannot be reached anyway because these nodes end their respective chains (see remark in the previous section).

Neurophysiological studies bring precious information on the possibility for short-range inhibitory loops between excitatory neurons and inhibitory interneurons [TLR16, YFP$^+$11]. Such biologically relevant connectivity allows for selective self-inhibition of excitatory neurons proportional to their level of excitation in computational models [DPT$^+$16, LBH$^+$21, VBS11]. This mechanism allows to circumvent the obstacle of too strong self excitation of excitatory populations, by counterbalancing the higher excitability of a unit k in (10) by a specific inhibitory term $-\nu_k x(k)$ on this unit. Here ν_k is roughly proportional to the number of afferent connections to excited units

that contribute to the activity of the inhibitory population k. Such selective self-inhibition is proportional to the excitation fed by the recurrent excitatory connections. More specifically we modify equation (5) by adding local self-inhibitory terms $\nu_i x_i$:

$$\begin{aligned}\dot{x_i} =& x_i(1-x_i)(-\mu x_i + \sum_{j=1}^{N} J_{i,j}^{max} s_j x_j \\ & - \lambda \sum_{j=1}^{N} x_j - \nu_i x_i - I) + \eta \end{aligned} \tag{10}$$

The coefficient ν_i has been chosen equal to $\lambda(d_i - 2)$ where d_i is the number of patterns sharing unit i if $d_i \geq 2$ and 0 otherwise.

3 Results

Computational modeling studies of priming in biologically inspired neural networks have shown that retrospective activity of a stimulus is possible for high values of synaptic efficacy between neurons that respond to this stimulus, which is coded in the model by the self excitation of the neurons population coding for the stimulus [AB97, ABY03]. Models further indicate that prospective activity of a stimulus predicted but not actually encoded is possible before it is presented for high values of synaptic efficacy between the populations of neurons coding for the two stimuli [Bru96, MAB03, LBS12, LS14]. Here we investigate how retrospective activity of a stimulus can generate the prospective activity of a given predicted stimulus selected among several possible predictions. We further investigate to what extent, at the current branching state, the branch taken by the network can be modified by modulating neuronal gain for a fixed connectivity matrix.

3.1 Latching dynamics in systems with multiple branches, case study

We consider two examples of networks with $N = 10$ units satisfying conditions H1 and H2 and with activities and synaptic dynamics s_i driven by Equations (10) and (1).

In the first case, the system encodes 9 patterns ξ^1 to ξ^9, which from now on, for the sake of clarity, we label with capital letters $A, B, ..., I$. These patterns are connected like in Fig. 3a. Any two consecutive units encode a pattern. Patterns ABC form the initial segment of the graph, patterns DEF and GHI form respectively the branches named Br-1 and Br-2. The connectivity matrix J^{max} is built according to Proposition 1. Note that the three patterns C, D and G share the active unit x_4. Therefore the coefficient

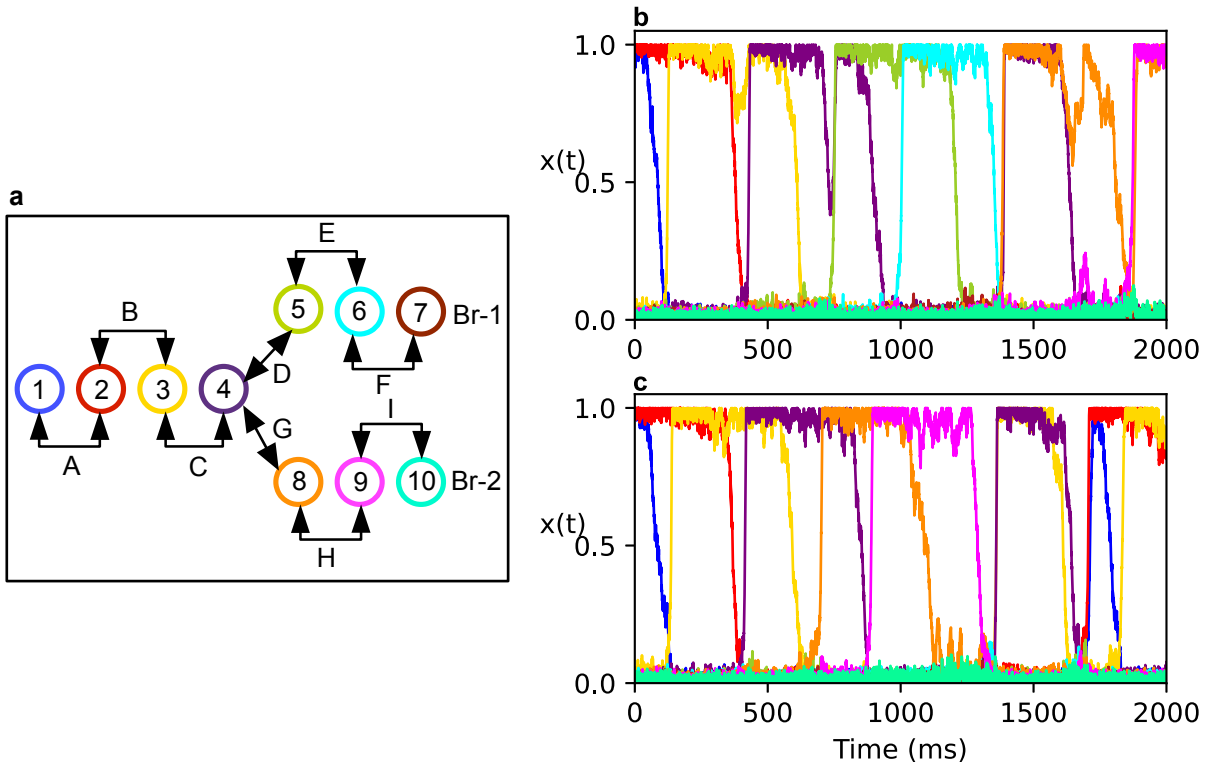


Figure 3: A system with a 3-ways branching. **a** Each numbered circle represents a unit. Two consecutive units encode a pattern. The excited unit 4 is shared by the three patterns C, D and G. When the system starts from pattern A in panel **a** it can follow either 'Br-1' (sequence takes the Br-1 direction) **b** or 'Br-2' (sequence takes the Br-2 direction) **c**. Parameters: $\tau_r = 300, \rho = 1.2, \lambda = 0.60, \mu = 0.40, \eta = 0.04$. Unit colour codes in **a** are respected in **b, c**.

$J^{max}_{4,4} = 3$ in the connectivity matrix. Therefore in (10) the coefficient of local self-inhibition $\nu_4 = 1$ while $\nu_i = 0$ if $i \neq 4$.

When (10) is initiated from the first pattern ξ^1, according to [KEAC$^+$20] the system follows the initial segment $A \to B \to C$. Then the value of ν_4 counterbalances the over excitation of unit x_4, which allows the system to continue along either branch Br-1 or Br-2. Figures 3b and 3c demonstrate the system taking regular forward sequences along Br-1 or Br-2, respectively. We also observe that after deactivation of x_6 in Fig. 3b and x_9 in Fig. 3c, irregular activations of encoded patterns proceed. Notice that neither the connectivity matrix nor the individual parameters imposes any preference between Br-1 and Br-2. Thus, we can expect equal probabilities for choosing one of these branches, in other words, an irregular behavior alternating randomly between the two branches. In order to investigate the persistence of this irregular behavior across parameter variations, we consider the parameter sets for which the system has a tendency to follow at least four patterns regularly, i.e. $\eta = 0.04, \mu \in \{0.30, 0.35, 0.40, 0.45, 0.5\}, \lambda \in \{0.55, 0.6, 0.65\}, \tau_r \in \{300, 900\}, \rho = \{1.2, 2.4\}$, (see [KEAC$^+$20] for details). We realized 800 simulations for each combinations.

Figure 4a-d summarises the probability of the different possible behaviors over all realisations, that is, the system can (or cannot) follow a forward regular sequence until the 3-ways branching at the unit 4 where it can stop, go back (called '0' state) or continue along Br-1 or Br-2. Having a high probability at '0' indicates the tendency of executing short sequences, which depends on λ, ρ, and τ_r. Chain length is longer for strong inhibition, e.g. $\lambda = 0.65$, for $(\rho, \tau_r) = (1.2, 900)$, but shorter for other combinations of (ρ, τ_r). For a sequence that crosses pattern C, the mean of the probability of choosing Br-1 and Br-2 are almost equal. In other words, the system has an equal probability of choice between Br-1 and Br-2. We note that in this case the choice is independent of μ (results not shown).

In our second case, the system has again $N = 10$ units which now encode 10 patterns $ABCDEFGHIJ$ (Fig. 5a). The additional pattern J is encoded by x_4 and x_{10}, so that the sequence $GHIJ$ forms a cycle. Now x_4 is the 4-ways branching point of the graph and participates in encoding patterns C, D, G and J. Thus, x_4 receives four excitatory inputs while the other intermediate units of the graph receive two. Taking the local self-inhibition parameter $\nu_4 = 2$ balances the over excitation on x_4.

In this configuration, a regular sequence initialized from pattern A can take three different forward direction at x_4: either moving along Br-1 (Fig. 5b), or entering the cycle in the forward direction by activating the pattern G (Cyc-f) (Fig. 5c), or entering the cycle in the backward direction by activating the pattern J (Cyc-b) (Fig. 5d). For Br-1 the system eventually stops its regular sequence at pattern E, then persuades an irregular activation of encoded patterns. On the other hand, if the system takes the cycle either in the forward or the backward directions, it can complete the cycle and reactivate x_4 at which it would again have three different options. For instance, in Fig.

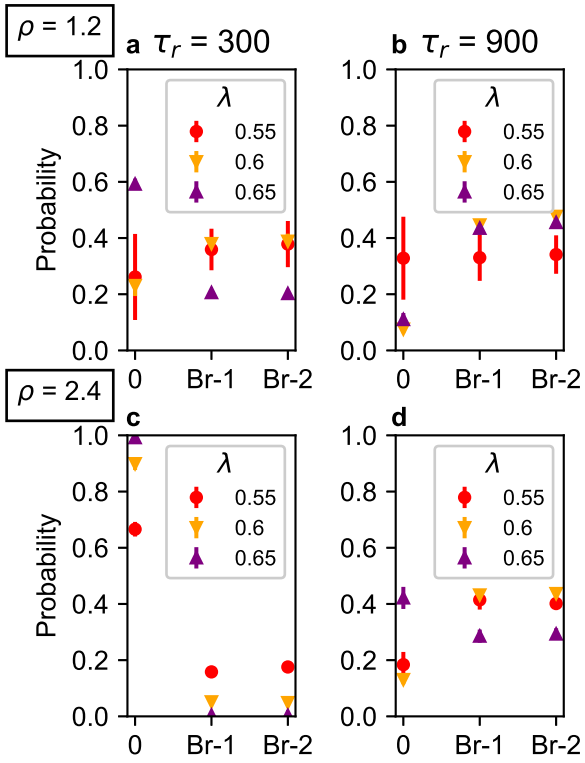


Figure 4: Probabilities of possible behaviors in the 3-ways branching system Fig. 3. **a-d** Error-bar plot of the probabilities of possible behaviors when the system starts from pattern A in Fig. 3**a**. The x-axis shows possible behaviours: '0' (sequence is either shorter than ABC, stopped at C, or takes the backward direction at C), 'Br-1' (sequence takes the Br-1 direction) and 'Br-2' (sequence takes the Br-2 direction). The y-axis shows the probability of each possible behaviour averaged over all realisations. Synaptic time constant equals to $\tau_r = 300$ on panels **a** and **c**, and $\tau_r = 900$ on panels **c** and **d**. **a, b** Probability of possible behaviours for $\rho = 1.2$. **c, d** Probability of possible behaviours for $\rho = 2.4$.

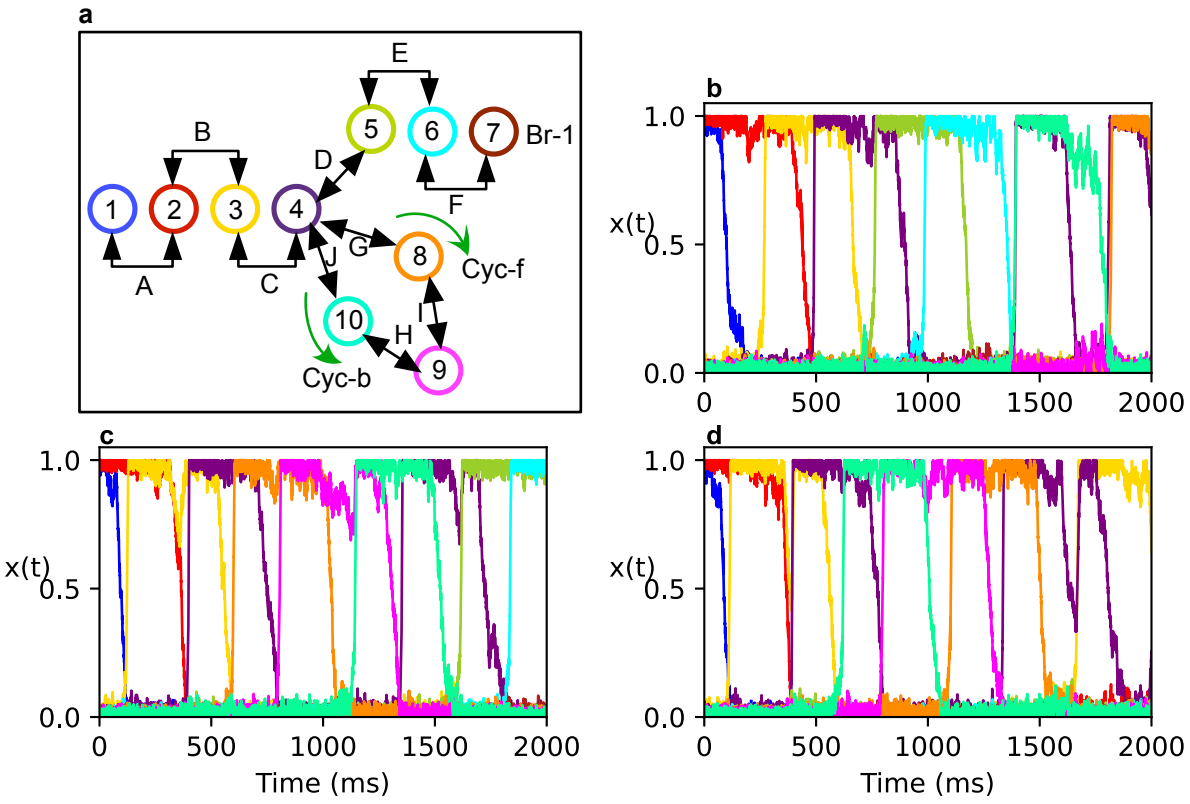


Figure 5: A system with a 4-ways branching point and a cycle. **a** Each numbered circle represents a unit (x_i). Two consecutive units encode a pattern. The unit 4 is a 4-ways branching point. When the system starts from pattern A in panel **a** it can follow 'Br-1' (sequence takes the Br-1 direction) **b**, Cyc-f' (sequence takes the forward cycle direction) **c**, or 'Cyc-b' (sequence takes the backward cycle direction) **d**. Parameters: $\tau_r = 300, \rho = 1.2, \lambda = 0.60, \mu = 0.40, \eta = 0.04$. Unit colour codes in **a** are respected in **b,c**.

5c, the system takes Cyc-f, completes the cycle along $GIHJ$, then follows Br-1. In Fig. 5d, the system takes Cyc-b, completes the cycle along $JHIG$, then follows the initial segment in backward direction. Once again, neither the system parameters nor the connectivity matrix imposes any preference in these choices. Choices are random and driven by noise. Therefore, we can expect a random behaviour with equal probability of taking any of Br-1, Cyc-f or Cyc-b if the system has a tendency to move on at x_4. Similar to our first case, the system can fail to move on when it reaches pattern C, so it can stop, or it can go backwards, or it can even fail to complete the initial segment. Since the system has more choices, we realised 1000 simulations for each parameter combinations. Figure 6a-d summarises possible behaviours over all realisations. Among the sequences that crosses the pattern C ('0' for the others), the system choices triggered by noise alone do not experience any preference among Br-1, Cyc-f or Cyc-b. As in the case of 3-nodes branching, the choice probability is independent of μ (results not shown).

3.2 Preference in a heterogeneous system

In the previous section, we have shown that the choice of predictions in a homogeneous and excitation/inhibition balanced system driven by noise is neutral, i.e. without any preference between branches. However, this neutrality can be biased by either a connectivity matrix that privileges a certain direction or the slope of the activation function μ that determines the sensitivity to excitation of the populations.

We then investigated the impact of heterogeneity in the system with a 3-ways branching point given in Fig. 4. As Fig. 7 shows, the system is neutral with the Hebbian-ruled (3) connectivity matrix and equal values of $\mu = 0.4$ for all units. When the units along Br-2 (units x_8, x_9 and x_{10}), have a different μ value, μ_{Br2}, the system takes more frequently the branch with lower μ values. In Fig. 7a,c this tendency is towards Br-2 for $\mu_{Br2} = 0.30$, whereas it is towards Br-1 in Fig. 7b,d for $\mu_{Br2} = 0.50$ (in both cases $\mu_{Br1} = 0.40$). This is intuitive because for an inactive unit the $(-\mu x_i)$ term in (10) acts like an inertia term (inverse of gain), and the unit should overcome this self-inertia to be activated.

The tendency towards the low-inertia branch (higher gain) can be tuned up or down by modifications of either the connectivity matrix or the neuronal gain $\gamma = 4/\mu$. If, for instance, x_8 with $\mu_{Br2} = 0.3$ receives stronger excitation from x_4 ($J^{max}_{8,4} = 1.05$), the probability of choosing Br-2 increases (square in Fig. 7a,c); whereas it decreases if x_8 receives less excitation, ($J^{max}_{8,4} = 0.95$, diamond in Fig. 7a,c). Figure 7e,f shows the impact of μ in a system where one of the branches is privileged by the connectivity matrix. Decreasing μ_{Br2} on the "synaptically unprivilege" branch can increase its chance to be chosen, whereas increasing μ_{Br2} reinforce the contrast between two branches. Interestingly, increasing μ_{Br2} along the privileged branch pushes the system towards the less excited branch. These results also in-

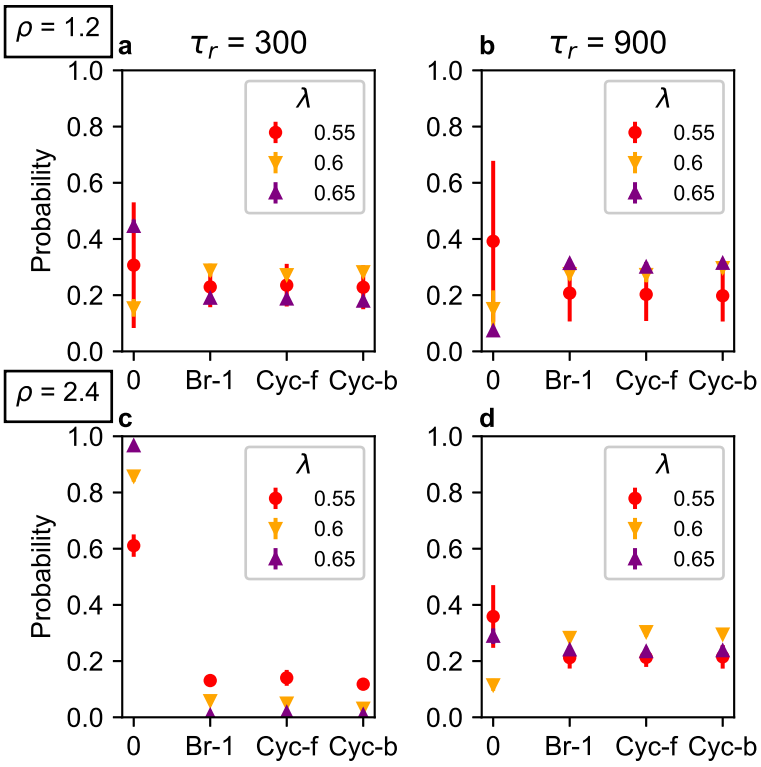


Figure 6: Probabilities of possible behaviours in the 4-ways branching system Fig. 5. **a-d** Error-bar plot of the probabilities of possible behaviours when the system starts from pattern A in Fig. 5**a**. The x-axis shows possible behaviours: '0' (sequence is either shorter than ABC, stopped at C, or takes a backward direction at C), 'Br-1' (sequence takes the Br-1 direction), 'Cyc-f' (sequence takes the forward cycle direction), and 'Cyc-b' (sequence takes the backward cycle direction). The y-axis shows the probability of each possible behaviour averaged over all realisations. Synaptic time constant equals to $\tau_r = 300$ on panels **a** and **c**, and $\tau_r = 900$ on panels **b** and **d**. **a, b** Probability of possible behaviours for $\rho = 1.2$. **c, d** Probability of possible behaviours for $\rho = 2.4$.

dicate that a preference for a branch introduced by the connectivity matrix can be tuned by adjusting neuronal gain $\gamma = 4/\mu$. Finally, the system does not execute a sequence along Br-2 for $\mu_{Br2} \geq \lambda$ (see App. A.1), which is a necessary condition for a transition from a unit i to $i + 1$. This condition is satisfied by x_4 since $\mu < \lambda$, but not by x_5 if $\mu_{Br2} \geq \lambda$.

4 Discussion

4.1 Effect of slow synaptic depression on Criticality

The results which have been presented in this report can be interpreted within the framework of the general concept of criticality and emerging phenomena. This concept originates from the study of complex systems in physical science and has shown to be insightful in neurosciences as well [Chi10]. There is indeed experimental evidence that the brain capability of interaction and adaptation with its environment, of decision making and cognitive functions, relies strongly on its ability to put itself in a near critical state [CGZB17]. Criticality refers here to the fact that the activity is neither trapped into an attractor state, like an equilibrium, out of which only very strong fluctuations would be able to drive the brain into another state, nor does it permanently evolve in a disordered manner, in which the dynamics would be driven by random fluctuations with no definite scale. These types of behavior depend on the parameters in the system and define regions in parameter space which are separated by an - in general - narrow region, in which the system exhibits transiently ordered states. These states, being not disordered, convey information which is expected to correspond to tasks operated by the brain. The present study has highlighted critical effects of synaptic and neuronal parameters of the network behavior such as feedback inhibition [MRL18], Hebbian learning of synaptic efficacy [BL98, MPC09] and activity-dependent synaptic depression [LH06]. Overall the network exhibits a self-organizing behavior combining several levels of criticality depending on these network parameters.

One question that arises when considering criticality is how does the brain proceed to be finely tuned so that it puts itself in a near critical state? Our previous work [KEAC$^+$20] highlighted the effect, seemingly not considered before, of the mechanism of slow synaptic depression combined with multistability. Initially the present network possesses a number P of stable steady-states, the learned states, which are associated with the connectivity matrix of synaptic strengths through a Hebbian learning process. Each learned state possesses a basin of attraction, that is, a domain surrounding it such that any trajectory starting in that domain converges asymptotically to it as time increases. This domain may be initially large and therefore the system is "far" from criticality. As time elapses, the synaptic efficacy of active neurons decreases up to the point at which the learned state becomes unstable

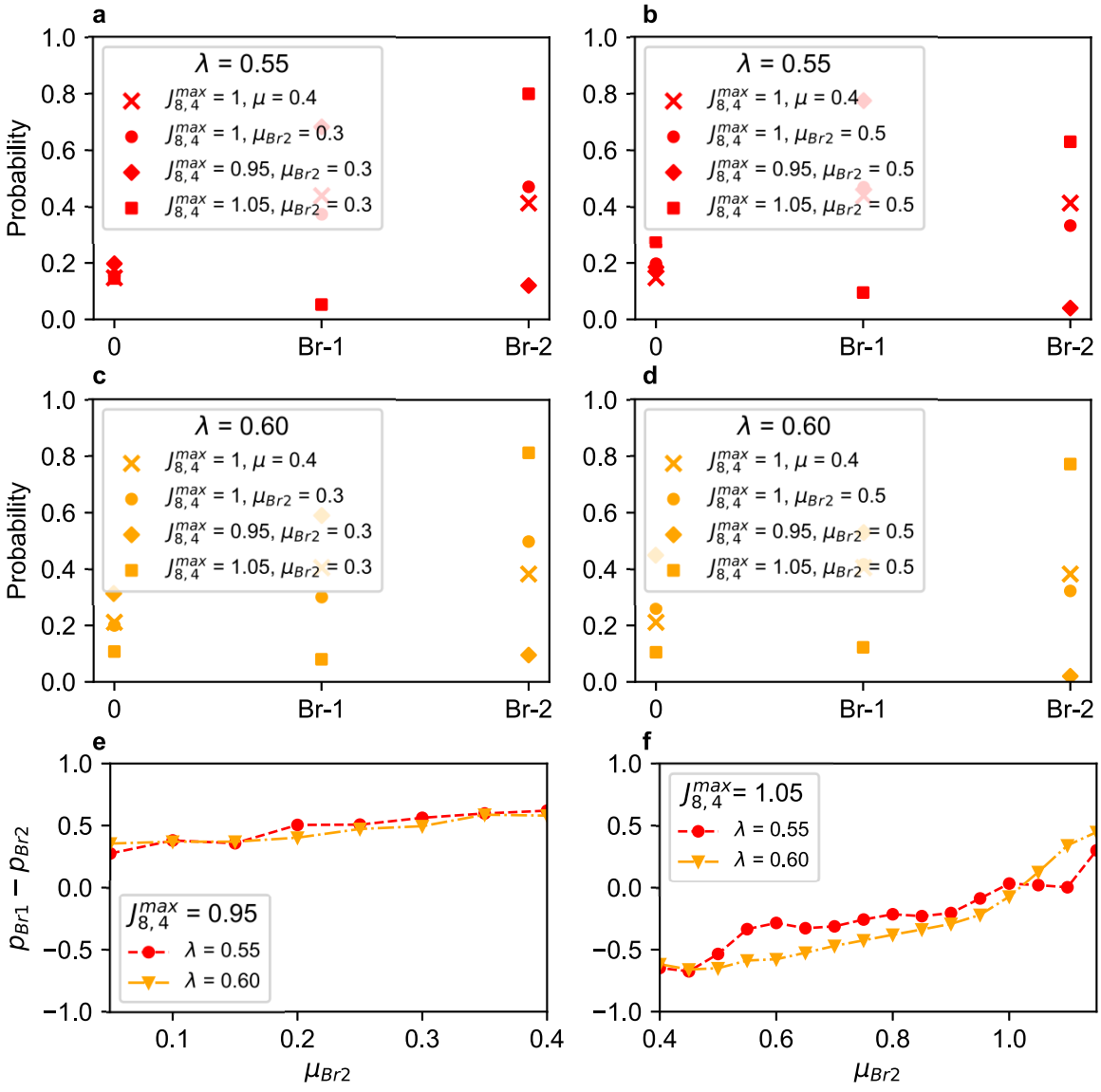


Figure 7: Impact of heterogeneity on choice probability in a system with a 3-ways branching point given in Fig. 4 with $(\rho, \tau_r) = (1.2, 300)$, $\lambda = 0.55$ on panels **a, b** and $\lambda = 0.60$ on panels **c, d**. Crosses for homogeneous network with $\mu = 0.4$. Two different gain values are considered for the units along Br-2 (units 8, 9 and 10): $\mu_{Br2} = 0.3$ (**a, c**) and $\mu_{Br2} = 0.5$ (**b, d**). Dots for the homogeneous synaptic gains, diamonds for weaker excitation from unit 4 to unit 8 ($J^{max}_{8,4} = 0.95$), and squares for stronger excitation from unit 4 to unit 8 ($J^{max}_{8,4} = 1.05$). Difference in probability of choosing Br-1 and Br-2, $p_{Br1} - p_{Br2}$, as a function of μ_{Br2} for $J^{max}_{8,4} = 0.95$ on panel **e** and for $J^{max}_{8,4} = 1.05$ on panel **f**.

or very weakly stable. Then the system reaches criticality. Under relatively small fluctuations it moves away and through a process which was explained in [KEAC$^+$20], it converges towards another learned state which shares an active unit (neuron) with the previous one. This process can repeat itself to form a sequence of jumps between the learned states (*latching dynamics*).

4.2 Effect of inhibition

Two types of inhibition are included in our model: global (non-selective) inhibition and local (selective) inhibition.

Our previous study [KEAC$^+$20] underlined that the global inhibition being in a suitable range increases the probability of long sequences. Indeed, this role is preserved in our extended model (Fig. 4, 6, 12). Yet, in our extended model the local inhibition is determinant for the regular chain length. In other words, if the excitation/inhibition balance is maintained by the local circuit, then predictions are guaranteed.

The local inhibition should be in an optimal range for the system to make a choice between several options (see App. A.3 and Fig. 12). Within this optimal range, the N-ways units can be deactivated by STD while keeping a window for exciting the associated units. Outside of it, either self excitation or self inhibition overcomes. In the former case, the system gets stuck at the most excited unit. In the latter, the system cannot maintain the patterns that the most excited unit involves. At the limit, the system is restricted to a sequence without the most excited unit. This mathematically intuitive mechanism can be physiologically plausible. Local inhibitory circuits have been reported to maintain the excitation/inhibition balance [TLR16] and their failure can cause pathological conditions [YFP$^+$11].

4.3 Effect of synaptic efficacy on prediction

In the present work, we considered the general case when a branching state can share an active unit with several other states orienting towards different branches. The chosen branch correspond to the prediction of a sequence of stimuli likely to occur in the environment. However, complex environments involve sequences of stimuli that occur with different frequencies. The present model shows that learning of sequences of different frequencies leads to a probabilistic choice of the system to move towards one or the other branch. Then, although prediction is useful to improve stimulus processing, it is prone to errors due to uncertainty in which sequence of stimuli will actually occur. The branch taken by the network can be a right or wrong prediction depending on the sequence of stimuli that actually occurs. To improve prediction success, the model is able to activate branches with probabilities that highly rely on the values of synaptic efficacy between the branching node and each branch. When two sequences of variable probability are embedded in the connectivity matrix, as expected the network takes more frequently the

branch that is the most strongly connected to the branching node. As a consequence, the network is able to select branches in proportion to the probability of the corresponding sequences: when the two branches have different probabilities, the model exhibits the lowest variability of choice by exploring more the more probable branch (Fig. 7a-d; rhombus *vs.* squares) and when the two branches have the same probability, the model exhibits the highest variability of choice by exploring the two branches with closer probability (Fig. 7a-d; crosses). In the example of the leopard, the issues after catching a prey, e.g. eating quietly or being disturbed, can have different probabilities. Learning hence leads to different values of synaptic efficacy between the branching node (the context of hunting for a prey) and each branch (the predictions of eating quietly or being disturbed). Stable learning of synaptic efficacy is beneficial to prediction in a stable environment, but it has limitations in environments that alternate between different local environments in space and/or time. In that case the difference in probability of the possible sequences of stimuli can be reversed. For example the passage of a group of scavengers through the leopard's territory transiently alters the likelihood of being disturbed during feeding compared to eating quietly. Alternation between local environments with reversed differences in probability confront the system to the problem of adapting quickly its predictions to new probabilities. Change in predictions could rely on rapid relearning and modification of the connectivity matrix. However, learning of the new probabilities would require a substantial amount of trial sequences in the environment and hence of predictions errors. In addition, the worst part of relearning is that it would lead to the forgetting of the probabilities involved in the previous environment, thus forcing a subsequent re-learning. The question is then how to change predictions transiently without forgetting, that is without modifications of the connectivity matrix?

4.4 Effect of neuronal gain on changes in prediction

The present study has investigated the effects of neuronal gain $\gamma = 4/\mu$ on the probability to take a branch or another, that is to predict one sequence of stimuli or another. Interestingly, results show that neuronal gain can alter the probability to select one or the other branch for a fixed matrix of synaptic efficacy.

The first case corresponds to the selective modulation of the gain of neurons coding states in one of the two branches (Fig. 7e-f). As expected, results show that the probability that the system takes a branch increases with the gain in this branch. This happens even though the strength of its connection to the branching node is stronger than the other branch (Fig. 7e). What was not expected is that modulation of the gain in the branch least associated with the branching node leads to an inversion of the respective probabilities of selecting the two branches, the less associated branch becoming more probable when the gain selectively increase in this branch (Fig. 7f).

The second case corresponds to the unselective modulation of the gain of all populations of neurons in the network, that is in the same way in the two branches. This case was studied because predictions of the effect of global changes in neuronal gain on all populations of neurons were not straightforward (see Fig. 8a-b). Interestingly, such unselective changes also lead to changes in the relative probability to select one or the other branch. As a consequence, unselective gain modulation can switch the network behavior between two strategies: a high difference in the probability of choosing the two possible branches and a low difference where the two branches are chosen more equally. The higher the gain the lower the contrast in the prediction of the two possible sequences, the lower the gain the higher the difference between the prediction of the two possible sequences (Fig. 8c).

The effects of gain modulation can change the probability with which the network generates different predictions on possible outcomes. The system can have either a regular behavior by generating more frequently the most probable sequence, or an irregular behavior by generating several sequences that have close frequencies. The exploration of different behaviors depends on the uncertainty about their issues [GU19, Ger19, DSTG20] and the variability of choices increases with the variability of rewards [BT93]. Considering that good choices bring rewards while bad choices do not, the maximization of rewards then requires the model to optimize the probability to take each branch according to rewards or errors given the actual sequences of stimuli. Changes in the local environment would then lead to changes in the probability of occurrence of the sequences of stimuli and changes in the ratio of rewards and errors. Experimental data on the link between precision of inferences and gain modulation [VWSM$^+$18] [TSL08] [GU19] suggest that changes in reward and prediction errors could modulate neuronal gain. Variations of neuronal gain are considered as depending on dopamine involved in reinforcement learning and decision making by reporting the precision of inferences [FDF15, FSF$^+$12]. The behavior of the present model shows that changes in neuronal gain lead to changes in the prediction strategy in alternating local environments:

- In the first place, a predictable local environment $E1$ would include a sequence of stimuli St_1 being more probable than the other St_2 (*e.g.* $P(St_1)$ = 0.70 *vs.* $P(St_2)$ = 0.30; Fig. 8c, case 1). In that case the system should predict the corresponding branch more frequently if not always (*e.g.* $P(Br\text{-}1)$ = 0.80 *vs.* $P(Br\text{-}2)$ = 0.20 for a 0.6 difference in probability for a low value of gain $\gamma = 4/\mu$ (high value of μ, Fig. 8a). The present study shows that the difference in prediction of the two branches depends on different parameters, including synaptic efficacy. For these values of probability of the sequences and of the branches predicted, the prediction strategy of high difference between predictions would bring more successes (62%) than errors (38%). A low neuronal gain would keep the system in this regular behavior of

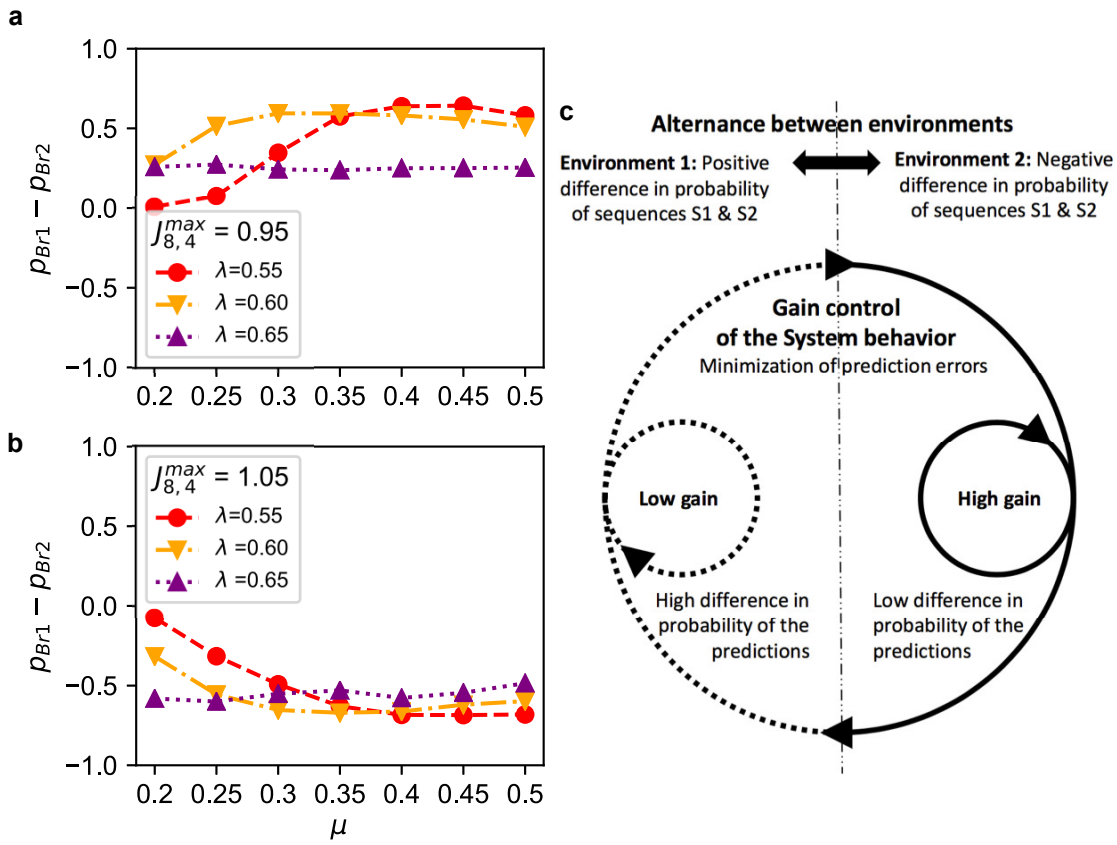


Figure 8: Effect of unselective changes of μ of all populations, for $J^{max}_{8,4} = 0.95$ in panel **a** and $J^{max}_{8,4} = 1.05$ in panel **b** for $(\rho, \tau_r) = (1.2, 300)$. **c** Gain modulation of the network behavior: the network can generate the two predictions with a high difference in probability (low gain) or a low difference in probability (high gain). This mechanisms allows for the minimization of prediction errors for a fixed connectivity matrix (see discussion).

predicting more frequently the more frequent sequence St_1 and maximize reward.

- Thereafter, a shift to another local environment $E2$ can lead to a reversal of the probabilities of the two sequences (*e.g.* $P(St_1)$ = 0.30 *vs.* $P(St_2)$ = 0.70; Fig. 8c, case 2). In this new environment, the preceding prediction strategy would increase errors (62%) at the expense of successes (38%). In that situation of increased errors, an increase of neuronal gain would shift the system behavior to become more regular and activate the predicted branches more equally (*e.g.* $P(Br\text{-}1)$ = 0.60 *vs.* $P(Br\text{-}2)$ = 0.40 for a 0.2 difference in the probability when the gain $\gamma = 4/\mu$ is high (low value of μ, Fig. 8a). For these values of probability of the sequences and of the branches predicted, the prediction strategy of low difference between predictions would increase successes (46%) and decrease errors (52%).
- A shift back to the initial environment $E1$ (*e.g.* $P(St_1)$ = 0.70 *vs.* $P(St_2)$ = 0.30) for similar probabilities of prediction of the two branches (*e.g.* $P(Br\text{-}1)$ = 0.60 *vs.* $P(Br-2)$ = 0.40) would lead to an increase of successes (54%) and a decrease of errors (46%). In that situation of increased reward, a decrease of neuronal gain would change the system behavior to become less regular and predict more the more probable sequence. The values of probability of the branches activated would come back to the initial values in the environment $E1$ (*e.g.* $P(Br\text{-}1)$ = 0.80 *vs.* $P(Br\text{-}2)$ = 0.20).

To summarize, dynamic changes in gain modulation make possible changes in the prediction strategy to minimize the costs of prediction errors in alternating local environments. The modulation of the gain allows to quickly adapt prediction strategy without forgetting by avoiding modifications of the synaptic efficiencies. In the example of the leopard with issues of different probabilities after catching a prey (*e.g.* eating quietly or being disturbed), predictions can adapt to rapid changes in the local environment through rapid modulation of the gain by rewards and errors.

However, we note that if the probabilities of the sequences are reversed between the two environments, the probabilities of the branches activated by the network should also be reversed. Here the modulation of the gain allows the network to shift between a high difference and a low difference between the branches activated. The resulting shift in strategy allows to minimize errors reward in transiently shifting environments, but not as efficiently in the environment with the difference in probability opposite to the difference in synaptic efficacy (*e.g.* $E2$) than in the environment with the difference in probability similar to the difference in synaptic efficacy (*e.g.* $E1$). If a new environment (*e.g.* $E2$) becomes stable for a longer time then the reversal of the probabilities of the branches activated would be made more durable through synaptic learning.

4.5 Conclusion

The model presented here shows how the combination of neural and synaptic parameters critically determine the choice of branches to predict learned sequences of stimuli. For a fixed learned matrix of synaptic efficacies, the difference in probability to activate a branch or the other can be reversed or decreased by modulation of neuronal gain at, respectively, the branch or network level. The ability to alternate between two prediction strategies is in accordance with priming strategies reported in human, with stronger activation when the environment is made of predictable words and weaker activation when the environment is less predictable [Nee91, LHK13, DBMLK17]. In other words, when predictions are successful in a predictable environment, the system continues to predict more strongly the more probable sequence, but when predictions fail in a less predictable environment, the system predicts less strongly the more probable sequence to "try" other sequences. The change in strategy would be triggered by the predictability of the local environment, which could rely on a reward-dependent dopaminergic coding of the precision of inferences in terms of prediction successes or errors. The present model identifies relations between changes in the probability of sequences in the environment and changes in the probability of the branches activated as predictions. This provide a framework for modeling and experimental approaches investigating the effects of rewards and errors of prediction on gain modulation and prediction strategies.

Declarations

Some journals require declarations to be submitted in a standardised format. Please check the Instructions for Authors of the journal to which you are submitting to see if you need to complete this section. If yes, your manuscript must contain the following sections under the heading 'Declarations':

- Conflict of interest: The authors declare that they have no conflict of interest.
- Ethics approval: Non applicable
- Consent to participate: Not applicable
- Consent for publication: Not applicable
- Availability of data and materials: Not applicable
- Code availability: Available at https://github.com/elifkoksal/dynamicBranching
- Authors' contributions: All authors contributed to the study conception, design, writing. All authors read and approved the final manuscript.
- Funding: The authors did not receive support from any organization for the submitted work.

A The latching dynamics

A.1 Sketch of the analysis in [KEAC$^+$20]

A sequence of $N-1$ learned patterns $\xi^i = (\xi^i_1 \ldots, \xi^i_N)$ was considered in a network of N units, where $\xi^k_i = \xi^k_{i+1} = 1$ and the other coordinates are 0. These patterns sit on vertices of the hypercube $[0,1]^N$ and the trajectories of the activity equations (5) lie within the hypercube. The analysis will be simplified by the presence of the factor $x_i(1-x_i)$ in (5), which forces the trajectories starting on one face of the hypercube to lie within that face, whatever the dimension of the face. In particular, the vertices are the steady-states of (5). The evolution of the system is governed by the activity equations (5) and the STD is driven by (1). The corresponding connectivity matrix is (7), according to the learning rule (3). In the following we sketch without proofs the analysis in [KEAC$^+$20].

The first question is about the stability of learned patterns ξ^i. This is determined by the sign of the eigenvalues at ξ^i of the Jacobian matrix of the system (5), which we write σ^i_j ($j = 1, \ldots, N$). These eigenvalues are easily computed because the edges emanating from ξ^i on the hypercube are the eigendirections. It can be seen that all eigenvalues with $j < i$ or $j > i+1$ are negative if the condition $2\lambda + I > S$ is satisfied ($S = (1+\rho)^{-1} < 1$ is the value towards which the synaptic strength s_i decays as time elapses). The two remaining eigenvalues are

$$\begin{aligned} \sigma^i_i &= \mu + 2\lambda + I - m s_i - s_{i+1} \\ \sigma^i_{i+1} &= \mu + 2\lambda + I - s_i - m' s_{i+1} \end{aligned} \tag{11}$$

where $m = 1$ if $i = 1$, $m' = 1$ if $i = N-1$, and $m = m' = 2$ for all other values of i.

Without STD the learned patterns ξ^i with $1 < i < N-1$ are stable under the mild condition $S < 2\lambda + I < 3 - \mu$. When $i = 1$ or $N-1$ the condition becomes $S < 2\lambda + I < 2 - \mu$, which is more restrictive. We assumed in [KEAC$^+$20] that $I = 0$. The results are still valid with $I > 0$ small enough. In this study we have set $I = 0$.

If STD is on, s_i and s_{i+1} decay towards $S < 1$, so that eventually σ^i_i or σ^i_{i+1} may become positive at finite time. When $i = 1$, (11) shows that $\sigma^1_1 > \sigma^1_2$, therefore ξ^i becomes first unstable and the direction of this instability is x_1. When $i > 1$, $m = m'$ in (11), so that σ^i_i and σ^i_{i+1} may become positive simultaneously. However, thanks to the previous switch $\xi^{i-1} \to \xi^i$, s_i has been decaying towards S while s_{i+1} was still close to 1 ($x_{i+1} = 0$ at ξ^{i-1}). Hence in any case ξ^i is first destabilized along x_i.

We claim that "typical" trajectories starting near ξ^i will converge towards ξ^{i+1} by first decreasing x_i towards 0, so that the trajectory converges for some time towards the *intermediate state* $\hat{\xi}^i = (0, 1, 0, \ldots, 0)$ (which represents the "overlap" between the learned patterns ξ^i and ξ^{i+1}), then increasing

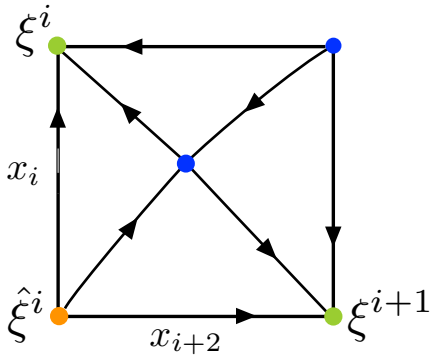


Figure 9: A typical phase portrait of the flow in the square F_i in the absence of synaptic depression. Green spots correspond to the learned patterns. Other spots are unstable steady-states.

x_{i+2} towards 1, so that ξ^{i+1} is reached. Noise is an essential ingredient of this behavior as we will see. The proof of the claim relies on the following properties of the system: **(i)** the synaptic variables s_j are slow compared to the activity variables x_j and can be seen, in the limit of "stationary variables", as bifurcation parameters for the x_j's. This is the idea of "dynamic bifurcation". These bifurcations drive the dynamics of the activity variables. **(ii)** The analysis can be restricted to the flow-invariant 2 dimensional face F_i on the hypercube, with vertices ξ^i, $\hat{\xi}^i$ and ξ^{i+1}. In F_i, $x_{i+1} = 1$, $x_j = 0$ when $j < i$ or $j > i+2$ and the coordinates are x_i, x_{i+2}. In these coordinates $\xi^i = (1,0)$, $\xi^{i+1} = (0,1)$ and $\hat{\xi}^i = (0,0)$.

Without synaptic plasticity, the learned patterns are stable and the dynamics in F_i looks like Fig. 9. When STD is on, synaptic strengths s_i of active neurons diminish slowly, which triggers successive transitions in F_i. The proof of the claim is provided in [KEAC$^+$20] and relies upon slow-fast dynamical systems theory. Here we only describe the possible scenarios.

The eigenvalue at ξ^i along coordinate x_i is given in (11) and note that $\hat{\xi}^i$ has a double eigenvalue in F_i, given by

$$\hat{\sigma}_i^i = \hat{\sigma}_{i+2}^i = -\lambda + s_{i+1} \tag{12}$$

Initially, ξ^i is stable. Let $t_{(1,0)}$ be the time at which $ms_i(t_{(1,0)}) + s_{i+1}(t_{(1,0)}) = \mu + 2\lambda$ so that σ_i^i becomes positive, and let $t_{0,0}$ be the time at which the initially positive eigenvalue $\hat{\sigma}_i^i$ becomes negative. This happens when $s_{i+1}(t_{(0,0)}) = \lambda$. Depending on the order of these two critical times two scenarios can occur.

Scenario 1: $t_{(1,0)} < t_{(0,0)}$. A (dynamic) bifurcation of a stable equilibrium occurs on the edge $x_{i+2} = 0$ from the equilibrium $(1,0)$. This equilibrium travels towards $(0,0)$, which is reached at time $t_{(0,0)}$. A trajectory starting

at initial time from the vicinity of $\xi^i = (1,0)$ will therefore follow the edge $x_{i+2} = 0$ until it arrives in a neighborhood of $\hat{\xi}^i$.

Scenario 2: $t_{(1,0)} > t_{(0,0)}$, so that an equilibrium bifurcates first from $(0,0)$ along the edge $x_{i+2} = 0$. The point $(1,0)$ is still stable but its basin of attraction shrinks. Then sufficient noise may allow the trajectory starting in the vicinity of $(1,0)$ to escape its basin of attraction and converge towards $\hat{\xi}^i$.

In both scenarios, in order for the trajectory to converge to ξ^{i+1}, one must have $\sigma_{i+2}^{i+1} < 0$, which by (11) requires $s_{i+1} + m' s_{i+2} > \mu + 2\lambda$. Since s_{i+2} is still close to 1 this condition is easily satisfied, as was seen above, unless $m' = 1$. In this case $i = N - 1$, which implies that the last pattern of the chain can hardly be attained by the system.

Additional constraints shared by the two scenarios must be satisfied, notably that $\hat{\xi}^i$ be stable in the transverse directions to F_i. This gives the condition $\mu < \lambda$.

A.2 Latching dynamics in the case of N-ways branching

We analyze how the presence of a multiple node in the graph of learned patterns affects the occurrence of latching dynamics. For the sake of clarity we concentrate on the example associated with the connectivity matrix (8), where the node ξ^2 has multiplicity 3 (Example 1, Section 2.2). The generalization to higher multiplicity is straightforward.

Now the equations for the neural activity are (10) where the term ν_i is 0 if $i \neq 3$ and $\nu_3 = \lambda$. Along chains which do not encounter the branching "choice" $\xi^2 \to \xi^3$ or $\xi^2 \to \xi^5$, the latching dynamics analysis proceeds as sketched in A.1. Indeed the higher excitation at unit 3, which in the factor of $x_i(1 - x_i)$ in (10) reads $3s_3x_3$, is compensated by the higher inhibition $-3\lambda x_3$. We therefore concentrate on the piece of the graph defined by the multi node ξ^2 and its adjacent patterns ξ^3 and ξ^5.

We expect ξ^2 becomes first unstable along its coordinate x_2, converging towards the intermediate state $\hat{\xi}^2 = (0,0,1,0,\ldots,0)$. But then either x_4 or x_6 should rise to 1 (transitions $\xi^2 \to \xi^3$ or $\xi^2 \to \xi^5$. Therefore we need to consider the cube F_3 defined by setting $x_3 = 1$ and $x_j = 0$ for $j \neq 2, 4, 6$. In F_3, $\xi^2 = (1,0,0)$, $\xi^3 = (0,1,0)$, $\xi^5 = (0,0,1)$ and $\hat{\xi}^2 = (0,0,0)$. The equations in F_3 are

$$\begin{aligned}
\dot{x_2} =& x_2(1-x_2)(-\mu x_2 - \lambda(x_2 + x_4 + x_6 + 1) \\
&+ 2s_2x_2 + s_3) \\
\dot{x_4} =& x_4(1-x_4)(-\mu x_4 - \lambda(x_2 + x_4 + x_6 + 1) \\
&+ s_3 + 2s_4x_4) \\
\dot{x_6} =& x_6(1-x_6)(-\mu x_6 - \lambda(x_2 + x_4 + x_6 + 1) \\
&+ s_3 + 2s_6x_6)
\end{aligned} \tag{13}$$

Observe that restricting further the equations to the squares defined by $x_4 = 0$ or $x_6 = 0$ leads to systems completely analogous to those in F_i in A.1, so

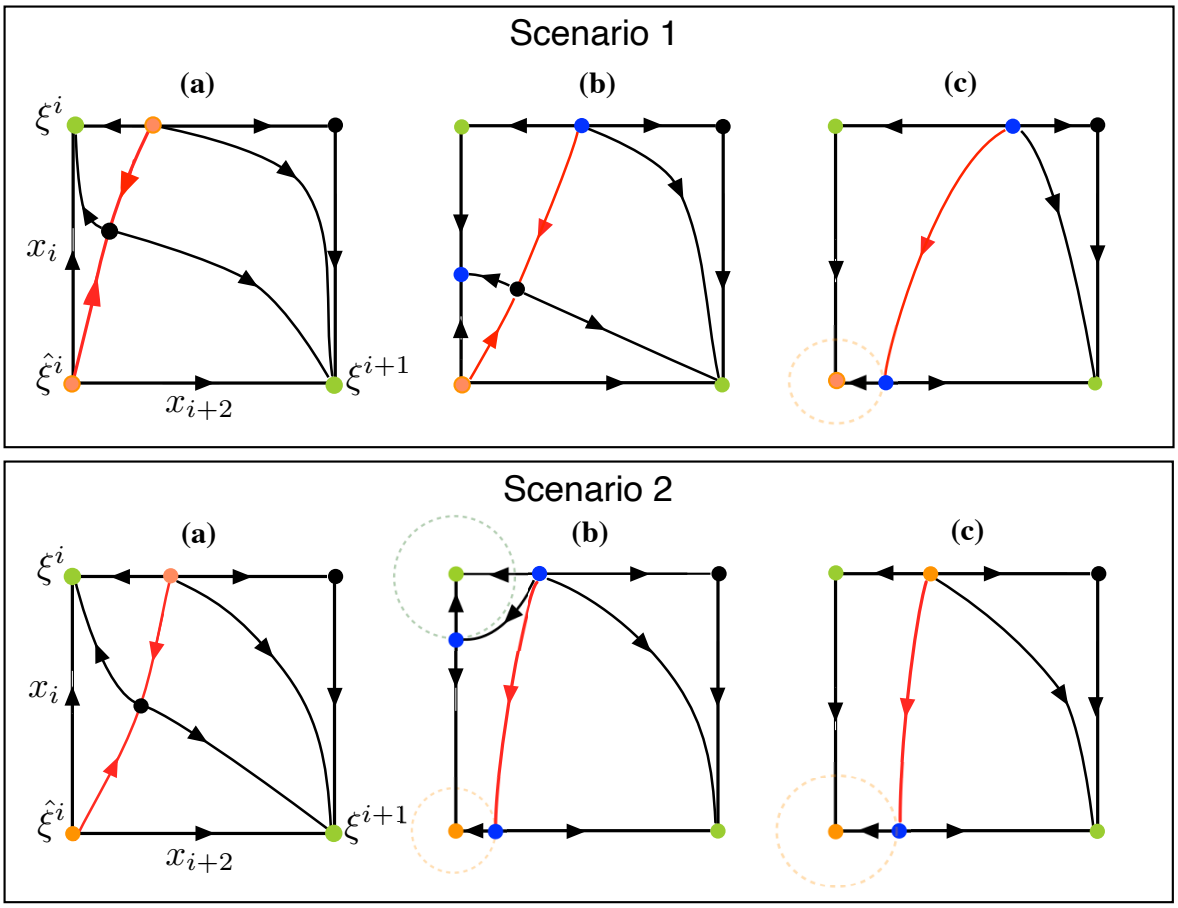


Figure 10: Snapshots of the transition $\xi^i \to \xi^{i+1}$ in the square F_i, in the scenarios 1 and 2. Bifurcated equilibria are blue. Red lines mark the boundary of the basin of attraction of ξ^{i+1} and dashed circles mark the closest distance for a possible stochastic jump over it. **Scenario 1**: (a) ξ^i is still stable. (b) Trajectory starting near ξ^i follows the saddle which has dynamically bifurcated on the edge $x_{i+2=0}$, until it reaches $\hat{\xi}^i$. Then arbitrary small noise can suffice to allow trajectory to jump towards ξ^{i+1}. (c) $\hat{\xi}^i$ has become stable by dynamic bifurcation of a saddle point on the edge $x_{i+2=0}$, but trajectory can jump over its basin of attraction by effect of sufficiently strong noise and then converge to ξ^{i+1}. **Scenario 2**: (a) same as scenario 1. (b) A saddle has bifurcated on the edge x_{i+2}, so that a trajectory starting near ξ^i can only converge to ξ^{i+1} by the effect of strong enough noise. (c) Eventually the trajectory can converge towards $\hat{\xi}^i$ and the same situation as in scenario 1 holds.

that the same analysis applies to both faces. Moreover the transverse eigenvalues to these faces at ξ^3 and ξ^5 are, in the notations of A.1, $\sigma_6^3 = \sigma_4^5 = -2\lambda + s_3 < 0$. Therefore the dynamics will closely follow one of the faces and the transitions $\xi^2 \to \xi^3$ and $\xi^2 \to \xi^5$ will occur with equal probability. Fig. 11 illustrates the global dynamics in F_3 in a case corresponding to scenarios 1-(c) or 2-(c) in Fig. 10.

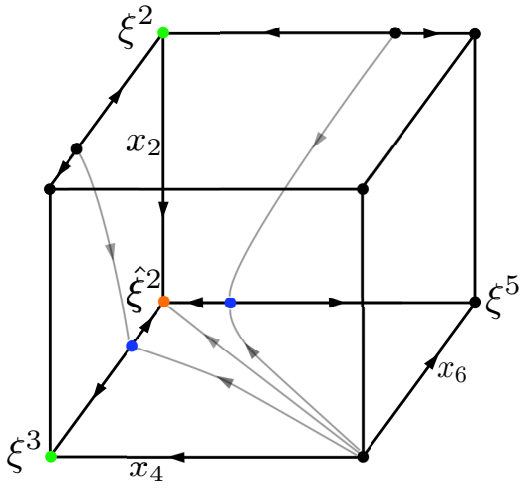


Figure 11: A sketch of the dynamics in F_3 corresponding to Fig. 10, scenario 1-(c) or scenario 2-(c).

A.3 Relation between the number of excitatory connections and self-inhibition

Consider that the system is in F_3 and $(x_2, x_4, x_6) = (1, 0, 0)$, which corresponds to ξ^2. As s_i variables varies in slow time, the system (13) will undergo several bifurcations that leading to either $\xi^2 \to \hat{\xi}^2 \to \xi^3$ or $\xi^2 \to \hat{\xi}^2 \to \xi^5$ transitions, with equal probabilities. The conditions for the $\xi^2 \to \hat{\xi}^2 \to \xi^3$ transition can be derived form the eigenvalue expressions:

- Initially stable equilibrium point $(x_2, x_4, x_6) = (1, 0, 0)$ becomes unstable at $t = t^3_{(1,0,0)}$:

$$2s_2(t^3_{(1,0,0)}) + s_3(t^3_{(1,0,0)}) = \mu + 2\lambda.$$

- Initially unstable equilibrium point $(x_2, x_4, x_6) = (0, 0, 0)$ becomes stable at $t = t^3_{(0,0,0)}$:

$$s_3(t^3_{(0,0,0)}) = \lambda.$$

The next transition is $\xi^3 \to \hat{\xi}^3 \to \xi^4$ in F_4 defined by setting $x_4 = 1$ and $x_j = 0$ for $j \neq 3, 5$. In F_4 the equations of the neural activity are reduced to

$$\begin{aligned}\dot{x_3} =& x_3(1-x_3)(-\mu x_3 - \lambda(x_3 + x_5 + 1) \\ & - \nu_3 x_3 + 3 s_3 x_3 + s_4) \\ \dot{x_5} =& x_5(1-x_5)(-\mu x_5 - \lambda(x_3 + x_5 + 1) \\ & - \nu_5 x_5 + s_4 + s_5 x_5)\end{aligned}$$

The conditions for the transition $\xi^3 \to \hat{\xi}^3 \to \xi^4$ are

- Initially stable equilibrium point $(x_3, x_5) = (1, 0)$ becomes unstable at $t = t^4_{(1,0)}$:

$$3 s_3(t^4_{(1,0)}) + s_4(t^4_{(1,0)}) = \mu + 2\lambda + \nu_3.$$

- Initially unstable equilibrium point $(x_3, x_5) = (0, 0)$ becomes stable at $t = t^4_{(0,0)}$:

$$s_4(t^4_{(0,0)}) = \lambda.$$

Assume that $t^3_{(1,0,0)} < t^3_{(0,0,0)}$ and $t^4_{(1,0)} < t^4_{(0,0)}$. To have equally distributed pattern durations along a sequence, the s_i values at the bifurcation moments should read $s_2(t^3_{(1,0,0)}) = s_3(t^4_{(1,0)})$ and $s_3(t^3_{(1,0,0)}) = s_4(t^4_{(1,0)})$. With this restriction, the following algebraic condition can be deduced:

$$\begin{aligned}2 s_3(t^4_{(1,0)}) + s_4(t^4_{(1,0)}) &= \mu + 2\lambda, \\ 3 s_3(t^4_{(1,0)}) + s_4(t^4_{(1,0)}) &= \mu + 2\lambda + \nu_3,\end{aligned}$$

that is

$$s_3(t^4_{(1,0)}) = \nu_3.$$

More generally, the relation between the number excitatory connections d_i and the level of self-inhibition ν_i is given by:

$$(d_i - 2) s_i(t_{(1,0)}) = \nu_i,$$

with $s_i(t_{(1,0)})$ being the value of s_i at the moment where a learned pattern changes stability.

To demonstrate the effect of the local inhibition to forward activation, we simulated the system of $N = 10$ (Fig. 4) by changing the ratio between the local inhibition at the branching point ($\nu_4 = k_4 \lambda$) and the global inhibition. Figure 12 shows the average chain length of a regular as a function of ν_4/λ for $\lambda = \{0.55, 0.60, 0.65\}$.

The system initialised from pattern A follows a chain of 3 patterns ABC as unit x_4 being the last activated unit. Unit x_4 triggers either pattern D (unit x_5) or pattern G (unit x_8) in the forward direction or pattern C (unit x_3) in the

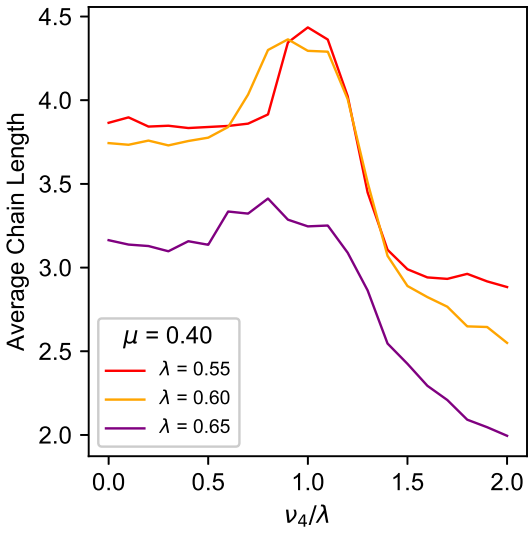


Figure 12: Average chain length versus the ratio between local ν_4 and global inhibition λ in the system of $N = 10$ (Fig. 4) for $\lambda = \{0.55, 0.60, 0.65\}$ and $\tau = 300, \rho = 1.2, \mu = 0.40, \eta = 0.40$.

backward direction. Eventually, the latter does not increase the chain length, but the formers do. However, if the local inhibition is not strong enough, unit x_4 stays active while patterns D and G die out due to the STD of the connections of units x_5 and x_8, respectively. Consequently, the following patterns cannot be activated. When the ν_4/λ ratio falls into an optimal range, unit x_4 can be deactivated early enough letting a window of excitation for patterns E and H. Interestingly, the optimal value of ν_4/λ is at 1 for $\lambda = 0.55$, then it is shifted leftwards for $\lambda = \{0.60, 0.65\}$ while the optimal range flattens.

We also observe that beyond the optimal range of ν_4/λ, the average chain length drops stiffly. For $\lambda = 0.55$, it stabilises around 3, which means that unit x_4 cannot sustain its activate state long enough for triggering patterns D and G. As the global inhibition increases, it becomes less and less unlikely that unit x_4 being activated and the chains shrink dramatically.

References

[AB97] D. J. Amit and N. Brunel. Model of global spontaneous activity and local structured activity during delay periods in the cerebral cortex. *Cerebral Cortex*, 7(3):237–52, 1997.

[ABOY12] A. Abraham, S. Beudt, D. V. M. Ott, and D. Yves von Cramon. Creative cognition and the brain: Dissociations between frontal, parietal–temporal and basal ganglia groups. *Brain Research*, 1482:55–70, 2012.

[ABT94] D. J. Amit, N. Brunel, and M. V. Tsodyks. Correlations of cortical hebbian reverberations: Theory versus experiment. *Journal of Neuroscience*, 14:6435–45, 1994.

[ABY03] D. J. Amit, A. Bernacchia, and V. Yakovlev. Multiple-object working memory–a model for behavioral performance. *Cerebral Cortex*, 13(5):435–43, 2003.

[AC05] G. Aston-Jones and J. D. Cohen. Adaptive gain and the role of the locus coeruleus–norepinephrine system in optimal performance. *Journal of Comparative Neurology*, 493(1):99–110, 2005.

[ACKL17] C. Aguilar, P. Chossat, M. Krupa, and F. Lavigne. Latching dynamics in neural networks with synaptic depression. *PLoS ONE*, 12(8):e0183710, 2017.

[ALA+19] C. Albrengues, F. Lavigne, C. Aguilar, E. Castet, and F. Vitu. Linguistic processes do not beat visuo-motor constraints, but they modulate where the eyes move regardless of word boundaries: Evidence against top-down word-based eye-movement control during reading. *PLoS ONE*, 14(7):e0219666, 2019.

[Ama72] S. Amari. Characteristics of random nets of analog neuron-like elements. *IEEE Transactions on systems, man, and cybernetics*, 5:643–57, 1972.

[BAHS08] R. L. Buckner, J. R. Andrews-Hanna, and D. L. Schacter. The brain's default network. *Annals of the New York Academy of Sciences*, 1124:1–38, 2008.

[BC93] T. V. Bliss and G. L. Collingridge. A synaptic model of memory: long-term potentiation in the hippocampus. *Nature*, 361:31–39, 1993.

[BC01] P. Bak and D. R. Chialvo. Adaptive learning by extrernal dynamics and negative feedback. *Physical Review E*, 63(3):031912, 2001.

[BKW+03] S. A. Bunge, I. Kahn, J. D. Wallis, E. K. Miller, and A.D. Wagner. Neural circuits subserving the retrieval and maintenance of abstract rules. *Journal of Neuophysiology*, 90(5):3419–28, 2003.

[BL73] T. V. Bliss and T. Lomo. Long-lasting potentiation of synaptic transmission in the dentate area of the anaesthetized rabbit following stimulation of the perforant path. *Journal of Physiology*, 232:331–56, 1973.

[BL98] E. Bienenstock and D. Lehmann. Regulated criticality in the brain? *Advances in Complex Systems*, 1(4):361–84, 1998.

[BL09] N. Brunel and F. Lavigne. Semantic priming in a cortical network model. *Journal of Cognitive Neuroscience*, 21(2300-19), 2009.

[BM05] C. V. Buhusi and W. H. Meck. What makes us tick? Functional and neural mechanisms of interval timing. *Nature Reviews Neuroscience*, 6(10):755–65, 2005.

[BP95] P. Bak and M. Paczuski. Complexity, contingency and criticality. *Proceedings of the National Academy of Sciences*, 92(15):6669–96, 1995.

[Bru96] N. Brunel. Hebbian learning of context in recurrent neural networks. *Neural Computation*, 15(8):1677–710, 1996.

[BSM+16] A. H. Bell, C. Summerfield, E. L. Morin, N. J. Malecek, and L. G. Ungerleider. Encoding of stimulus probability in macaque inferior temporal cortex. *Current Biology*, 26(17):2280–90, 2016.

[BT93] J. R. Busemeyer and J. T. Townsend. Decision field theory: a dynamic-cognitive approach to decision making in an uncertain environment. *Psychological Review*, 100(3):432, 1993.

[BW01] N. Brunel and X. J. Wang. Effects of neuromodulation in a cortical network model of object working memory dominated by recurrent inhibition. *Journal of Computational Neuroscience*, 11(1):63–85., 2001.

[CC01] C. M. Conway and M. H. Christiansen. Sequential learning in non-human primates. *Trends in Cognitive Sciences*, 5(12):539–46, 2001.

[CGS+09] K. Christoff, A. M. Gordon, J. Smallwood, R. Smith, and J. W. Schooler. Experience sampling during fmri reveals default network and executive system contributions to mind wandering. *Proceedings of the National Academy of Sciences*, 106(21):8719–24, 2009.

[CGZB17] L. Cocchi, L. L. Gollo, A. Zalesky, and M. Breakspear. Criticality in the brain: A synthesis of neurobiology, models and cognition. *Progress in Neurobiology*, 158:132–52, 2017.

[Chi10] D. R. Chialvo. Emergent complex neural dynamics. *Nature Physics*, 6(10):744–50, 2010.

[CM20] B. Chen and P. Miller. Attractor-state itinerancy in neural circuits with synaptic depression. *Journal of Mathematical Neuroscience*, 10(1):1–19, 2020.

[DBMLK17] N. Delaney-Busch, E. Morgan, E. F. Lau, and G. R. Kuperberg. Comprehenders rationally adapt semantic predictions to the statistics of the local environment: a Bayesian model of trial-by-trial N400 amplitudes. In *39th Annual Conference of the Cognitive Science Society*, London, England, 2017.

[DMZ+15] N. Ding, L. Melloni, H. Zhang, X. Tian, and D. Poeppel. ortical tracking of hierarchical linguistic structures in connected speech. *Nature Neuroscience*, 19(1):158–64, 2015.

[DPT+16] N. Dehghani, A Peyrache, B. Telenczuk, M. Le Van Quyen, E. Halgren, and S. S. et al. Cash. Dynamic balance of excitation and inhibition in human and monkey neocortex. *Scientific Reports*, 6(1):23176, 2016.

[DSTG20] I. Dasgupta, E. Schulz, J. B. Tenenbaum, and S. J. Gershman. A theory of learning to infer. *Psychological Review*, 127(3):412, 2020.

[DUK05] K. A. DeLong, T. P. Urbach, and M. Kutas. Probabilistic word pre-activation during language comprehension inferred from electrical brain activity. *Nature Neuroscience*, 8(8):1117–21, 2005.

[ED99] C. A. Erickson and R. Desimone. Responses of macaque perirhinal neurons during and after visual stimulus association learning. *Journal of Neuroscience*, 19(10404-16), 1999.

[ED12] S. L. Eagleman and V. Dragoi. Image sequence reactivation in awake v4 networks. *Proceedings of the National Academy of Sciences of the United States of America*, 109(47):450–55, 2012.

[FA71] J. M. Fuster and G. E. Alexander. Neuron activity related to short-term memory. *Science*, 173(3997):652–4, 1971.

[FB12] A. Fink and M. Benedek. EEG alpha power and creative ideation. *Neuroscience and Biobehavioral Reviews*, 44:11–123, 2012.

[FDF15] T. FitzGerald, R. J. Dolan, and K. J. Friston. Dopamine, reward learning, and active inference. *Frontiers in Computational Neuroscience*, 9:136, 2015.

[FNK+10] R. Fujimichi, Y. Naya, K. W. Koyano, M. Takeda, D. Takeuchi, and Y. Miyashita. Unitized representation of paired objects in area 35 of the macaque perirhinal cortex. *Europen Journal of Neuroscience*, 32(4):659–67, 2010.

[FSF+12] K. J. Friston, T. Shiner, T. FitzGerald, J. M. Galea, R. Adams, H. Brown, R.J. Dolan, R. Moran, Stephan K.E., and S. Bestmann. Dopamine, affordance and active inference. *PLoS Computational Biology*, 8(1):e1002327, 2012.

[GCD+94] P. M. Gochin, M. Colombo, G. A. Dorfman, G. L. Gerstein, and C. G. Gross. Neural ensemble coding in inferior temporal cortex. *Journal of Neuophysiology*, 71:2325–37, 1994.

[Ger19] S. J. Gershman. How to never be wrong. *Psychonomic Bulletin and Review*, 26(1):13–28, 2019.

[GU19] S. J. Gershman and N. Uchida. Believing in dopamine. *Nature Review Neuroscience*, 20(11):703–14, 2019.

[Gui50] J. P. Guilford. Creativity. *American Psychologist*, 5:444–54, 1950.

[GYdSL+13] G. Gonen-Yaacovi, L.C. de Souza, R. Levy, M. Urbanski, G. Josse, and E Volle. Rostral and caudal prefrontal contributions to creativity: a meta-analysis of functional imaging data. *Frontiers in Human Neuroscience*, 7:465, 2013.

[Heb49] D.O. Hebb. *The Organization of Behavior: A Neuropsychological Theory*. Wiley and Sons, New York, NY, 1949.

[HG12] H Harnal and A. L. Giraud. Cortical oscillations and sensory predictions. *Trends in Cognitive Science*, 16:390–8, 2012.

[HHNT14] K. Hutchison, S.J. Heap, J. Neely, and M. Thomas. Attentional control and asymmetric associative priming. *Journal of Experimental Psychology: Learning, Memory, and Cognition*, 40(3):844–56, 2014.

[HKP05] C. Hung, G. Kreiman, and J. Poggio, T. andDiCarlo. Fast read-out of object information in inferior temporal cortex. *Science*, 310:863–6, 2005.

[Hop82] J. J. Hopfield. Neural networks and physical systems with emergent collective computational abilities. *Proceedings of the National Academy of Sciences*, 79(8):2554–58, 1982.

[IQF15] M. J. Ison, Q. R. Quian, and I. Fried. Rapid encoding of new memories by individual neurons in the human brain. *Neuron*, 87(1):220–30, 2015.

[KB94] A. Kirkwood and M. F. Bear. Homosynaptic long-term depression in the visual cortex. *Neuroscience*, 14:3404–12, 1994.

[KDS11] M. Kutas, K. A. DeLong, and N. J. Smith. *Predictions in the Brain: Using Our Past to Generate a Future*, chapter A Look around at What Lies Ahead: Prediction and Predictability in Language Processing, pages 190–207. Oxford University Press, 2011.

[KEAC+20] E. Köksal-Ersöz, C. Aguilar, P. Chossat, M. Krupa, and F. Lavigne. Neuronal mechanisms for sequential activation of memory items: Dynamics and reliability. *PLoS ONE*, 15(4):e0231165, 2020.

[KHK+06] G. Kreiman, C. P. Hung, A. Kraskov, Q.R. Quian, T. Poggio, and J. J. DiCarlo. Object selectivity of local field potentials and spikes in the macaque inferior temporal cortex. *Neuron*, 49:433–45, 2006.

[Kri08] J. L. Krichmar. The neuromodulatory system: a framework for survival and adaptive behavior in a challenging world. *Adaptive Behavior*, 16(6):385–99, 2008.

[KW04] K. P. Körding and D. M. Wolpert. Bayesian integration in sensorimotor learning. *Nature*, 427(6971):244–7, 2004.

[LAD14] F. Lavigne, F. Avnaïm, and L. Dumercy. Inter-synaptic learning of combination rules in a cortical network model. *Frontiers in Psychology*, 5:842, 2014.

[Lav04] F. Lavigne. Aim networks: autoincursive memory networks for anticipation toward learned goals. *International Journal of Computing Anticipatory Systems*, 14:196–214, 2004.

[LBH+21] N.H. Lam, T. Borduqui, J. Hallak, A. C. Roque, A. Anticevic, and J. H. et al. Krystal. Effects of altered excitation-inhibition balance on decision making in a cortical circuit model. *Journal of Neuroscience*, 2021.

[LBS12] I. Lerner, S. Bentin, and O. Shriki. Spreading activation in an attractor network with latching dynamics: automatic semantic priming revisited. *Cognitive Science*, 36:1339–82., 2012.

[LCDV13] F. Lavigne, L. Chanquoy, L. Dumercy, and F. Vitu. Early dynamics of the semantic priming shift. *Advances in Cognitive Psychology*, 9(1):1–14, 2013.

[LD02] F. Lavigne and S. Denis. Neural network modeling of learning of contextual constraints on adaptive anticipations. *International Journal of Computing Anticipatory Systems*, 12:253–68, 2002.

[LD08] F. Lavigne and N. Darmon. Dopaminergic neuromodulation of semantic priming in a cortical network model. *Neuropsychologia*, 46:3074–87, 2008.

[LDC+12] F. Lavigne, L. Dumercy, L. Chanquoy, B. Mercier, and F. Vitu-Thibault. Dynamics of the semantic priming shift: Behavioral experiments and cortical network model. *Cogitive Neurodynamics*, 6(6):467–83, 2012.

[LDD11] F. Lavigne, L. Dumercy, and N. Darmon. Determinants of multiple semantic priming: A meta-analysis and spike frequency adaptive model of a cortical network. *Journal of Cognitive Neuroscience*, 23(6):1447–74, 2011.

[LH06] A. Levina and M. Herrmann. *Advances in Neural Information Processing Systems*, chapter Dynamical synapses give rise to

a power-law distribution of neuronal avalanches, pages 771–78. Number 18. MIT Press, Cambridge, MA, USA, 2006.

[LHK13] E. F. Lau, P. J. Holcomb, and G. R. Kuperberg. Dissociating N400 effects of prediction from association in single-word contexts. *Journal of Cognitive Neuroscience*, 25(3):484–502, 2013.

[LKD+07] C. C. Lapish, S. Kroener, D. Durstewitz, A. Lavin, and J. K. Seamans. The ability of the mesocortical dopamine system to operate in distinct temporal modes. *Psychopharmacology*, 191(3):609–25, 2007.

[LML21] L. Lazartigues, F. Mathy, and F. Lavigne. Statistical learning of unbalanced exclusive-or temporal sequences in humans. *PLoS ONE*, 16(2):e0246826., 2021.

[LR14] S. C. Li and A. Rieckmann. Neuromodulation and aging: implications of aging neuronal gain control on cognition. *Current Opinion on Neurobiology*, 29:148–58, 2014.

[LS14] I. Lerner and O. Shriki. Internally and externally driven network transitions as a basis for automatic and strategic processes in semantic priming: theory and experimental validation. *Frontiers in Psychology*, 5(314):00314, 2014.

[LVd00] F. Lavigne, F. Vitu, and G. d'Ydewalle. The influence of semantic context on initial eye landing sites in words. *Acta Psychologica*, 104(2):191–214, 2000.

[LVP14] B. J. Luka and C. Van Petten. Prospective and retrospective semantic processing: Prediction, time, and relationship strength in event-related potentials. *Brain and Language*, 135:115–29, 2014.

[MAB03] G. Mongillo, D. J. Amit, and N. Brunel. Retrospective and prospective persistent activity induced by hebbian learning in a recurrent cortical network. *Europen Journal of Neuroscience*, 18(7):2011–24, 2003.

[MC88] Y. Miyashita and H. S. Chang. Neuronal correlate of pictorial short-term memory in the primate temporal cortex. *Nature*, 331:68–70, 1988.

[MF12] K. D. Miller and F. Fumarola. Mathematical equivalence of two common forms of firing rate models of neural networks. *Neural Computation*, 24(1):25–31, 2012.

[MFR16] L. Minier, J. Fagot, and A. Rey. The temporal dynamics of regularity extraction in non-human primates. *Cognitive Science*, 40(4):1019–30., 2016.

[Mil99] E. K. Miller. The prefrontal cortex: complex neural properties for complex behavior. *Neuron*, 22:15–17, 1999.

[Miy88] Y. Miyashita. Neuronal correlate of visual associative long-term memory in the primate temporal cortex. *Nature*, 335, 1988.

[MPC09] M. O. Magnasco, O. Piro, and G. A. Cecchi. Self-tuned critical anti-Hebbian networks. *Physical Review Letters*, 102(25):258102, 2009.

[MRL18] G. Mongillo, S. Rumpel, and Y. Loewenstein. Inhibitory connectivity defines the realm of excitatory plasticity. *Nature Neuroscience*, 21(10):1463–70, 2018.

[MSZA01] A. Messinger, L.R. Squire, S. M. Zola, and T. D. Albright. Neuronal representations of stimulus associations develop in the temporal lobe during learning. *Proceedings of the National Academy of Sciences*, 98(12239-44), 2001.

[MWM06] R. Muhammad, J. D. Wallis, and E. K. Miller. A comparison of abstract rules in the prefrontal cortex, premotor cortex, inferior temporal cortex and striatum. *Journal of Cognitive Neuroscience*, 18(6):974–89, 2006.

[Nee91] J. H. Neely. *Basic processes in reading: Visual word recognition*, chapter Semantic priming effects in visual word recognition: A selective review of current findings and theories, pages 264–336. Lawrence Erlbaum Associates, Inc., 1991.

[NYM01] Y. Naya, M. Yoshida, and Y. Miyashita. Backward spreading of memory-retrieval signal in the primate temporal cortex. *Science*, 291(5504):661–64, 2001.

[QK10] Q. R. Quian and G. Kreiman. Measuring sparseness in the brain: comment on Bowers. *Psychological Review*, 117:291–99, 2010.

[Qui12] Q. R. Quian. Concept cells: the building blocks of declarative memory functions. *Nature Review Neuroscience*, 13:587–97, 2012.

[Qui16] Q. R. Quian. Neuronal codes for visual perception and memory. *Neuropsychologia*, 83:227–41, 2016.

[RG06] P. Redgrave and K. Gurney. The short-latency dopamine signal: a role in discovering novel actions? *Nature Review Neuroscience*, 7(12):967–75, 2006.

[RLDW08] E. T. Rolls, M. Loh, G. Deco, and G. Winterer. Computational models of schizophrenia and dopamine modulation in the prefrontal cortex. *Nature Review Neuroscience*, 9:696, 2008.

[RNTK08] E. Russo, V. M. Namboodiri, A. Treves, and E. Kropff. Free association transitions in models of cortical latching dynamics. *New Journal of Physics*, 10(1):015008, 2008.

[RRM99] G. Rainer, S. C. Rao, and E. K. Miller. Prospective coding for objects in primate prefrontal cortex. *Journal of Neuroscience*, 19:5493–5505, 1999.

[RT95] E. T. Rolls and M. J. Tovee. Sparseness of the neuronal representation of stimuli in the primate temporal visual cortex. *Journal of Neuophysiology*, 73(2):713–26, 1995.

[SM91] K. Sakai and Y. Miyashita. Neural organization for the long-term memory of paired associates. *Nature*, 354:152–55, 1991.

[TFTL06] D. Y. Tsao, W. A. Freiwald, R. B. Tootell, and M. Livingstone. A cortical region consisting entirely of face-selective cells. *Science*, 311(5761):670–4, 2006.

[TLR16] R. Tremblay, S. Lee, and B. Rudy. GABAergic interneurons in the neocortex: From cellular properties to circuits. *Neuron*, 91:260–92, 2016.

[TM97] M. V. Tsodyks and H. Markram. The neural code between neocortical pyramidal neurons depends on neurotransmitter release probability. *Proceedings of the National Academy of Sciences*, 94:719–23, 1997.

[Tre05] A. Treves. Frontal latching networks: a possible neural basis for infinite recursion. *Cognitive Neuropsychology*, 22(3-4):276–91, 2005.

[TSL08] K. Thurley, W. Senn, and H. R. Luscher. Dopamine increases the gain of the input-output response of rat prefrontal pyramidal neurons. *Journal of Neurophysiology*, 99(6):2985–97, 2008.

[Tso90] M. V. Tsodyks. Hierarchical associative memory in neural networks with low activity level. *Modern Physics Letters B*, 4:259–65, 1990.

[TT01] H. Tamura and K. Tanaka. Visual response properties of cells in the ventral and dorsal parts of the macaque inferotemporal cortex. *Cerebral Cortex*, 11:384–99, 2001.

[VBS11] V. Volman, M. M. Behrens, and T. J. Sejnowski. Downregulation of parvalbumin at cortical GABA synapses reduces network gamma oscillatory activity. *Journal of Neuroscience*, 31(49):18137–48, 2011.

[VCSJK15] A. Veliz-Cuba, H. Z. Shouval, K. Josic, and Z.P. Kilpatrick. Networks that learn the precise timing of event sequences. *Journal of Computational Neuroscience*, 39:235–54, 2015.

[VP14] C. Van Petten. Examining the N400 semantic context effect item-by-item: Relationship to corpus-based measures of word co-occurrence. *International Journal of Psychophysiology*, 94:407–19, 2014.

[VSG+97] J. A. Varela, K. Sen, J. Gibson, J. Fost, L. Abbott, and S. B. Nelson. A quantitative description of short-term plasticity at excitatory synapses in layer 2/3 of rat primary visual cortex. *Journal of Neuroscience*, 17(20):7926–40, 1997.

[VWSM+18] C. M. Vander Weele, C. A. Siciliano, G. A. Matthews, P. Namburi, E. M. Izadmehr, I. C. Espinel, E. H. Nieh, E. Schut, N. Padilla-Coreano, A. Burgos-Robles, C. J. Chang, E. Y. Kimchi, A. Beyeler, R. Wichmann, C. P. Wildes, and K. M. Tye. Dopamine enhances signal-to-noise ratio in cortical-brainstem encoding of aversive stimuli. *Nature*, 563:397–401, 2018.

[WAM01] J. D. Wallis, K. C. Anderson, and E. K. Miller. Single neurons in prefrontal cortex encode abstract rules. *Nature*, 411(6840):953–6, 2001.

[Wan02] X.J. Wang. Probabilistic decision making by slow reverberation in cortical circuits. *Neuron*, 36:955–68, 2002.

[WC12] H. R. Wilson and J. D. Cowan. Excitatory and inhibitory interactions in localized populations of model neurons. *Biophysics Journal*, 12(1):1–24, 2012.

[Wei98] N. M. Weinberger. Physiological memory in primary auditory cortex: characteristics and mechanisms. *Neurobiology of Learning and Memory*, 70(1-2):226–51, 1998.

[WFN+15] R. M. Willems, S. L. Frank, A. D. Nijhof, Hagoort P., and A. van den Bosch. Prediction during natural language comprehension. *Cerebral Cortex*, 26(6):2506–16, 2015.

[WM03] J. D. Wallis and E. K. Miller. From rule to response: neuronal processes in the premotor and prefrontal cortex. *Journal of Neuophysiology*, 90(3):1790–806, 2003.

[WYF+03] S. Wirth, M. Yanike, L. M. Frank, A. C. Smith, E.N. Brown, and W.A. Suzuki. Single neurons in the monkey hippocampus and learning of new associations. *Science*, 300(5625):1578–81, 2003.

[XJP12] S. Xu, W. Jiang, and M. Dan Y. Poo. Activity recall in a visual cortical ensemble. *Nature Neuroscience*, 15:449–55, 2012.

[YFEE98] V. Yakovlev, S. Fusi, Berman. E., and Zohary. E. nter-trial neuronal activity in inferior temporal cortex: a putative vehicle to generate long-term visual associations. *Nature Neuroscience*, 1(4):310–17, 1998.

[YFP+11] O. Yizhar, L.E. Fenno, M. Prigge, F. Schneider, T.J. Davidson, and D. J. et al. O'Shea. Neocortical excitation/inhibition balance in information processing and social dysfunction. *Nature*, 477(7363):171–8, 2011.

[YNM03] M. Yoshida, Y. Naya, and Y. Miyashita. Anatomical organization of forward fiber projections from area TE to perirhinal neurons representing visual long-term memory in monkeys. *Proceedings of the National Academy of Sciences*, 100(4257-62), 2003.

[YY92] M. Young and S. Yamane. Sparse population coding of faces in the inferotemporal cortex. *Science*, 256(5061):1327–31, 1992.